Material Matters™

Vol. 4, No. 3

ALDRICH® Chemistry

Organic and Molecular Electronics

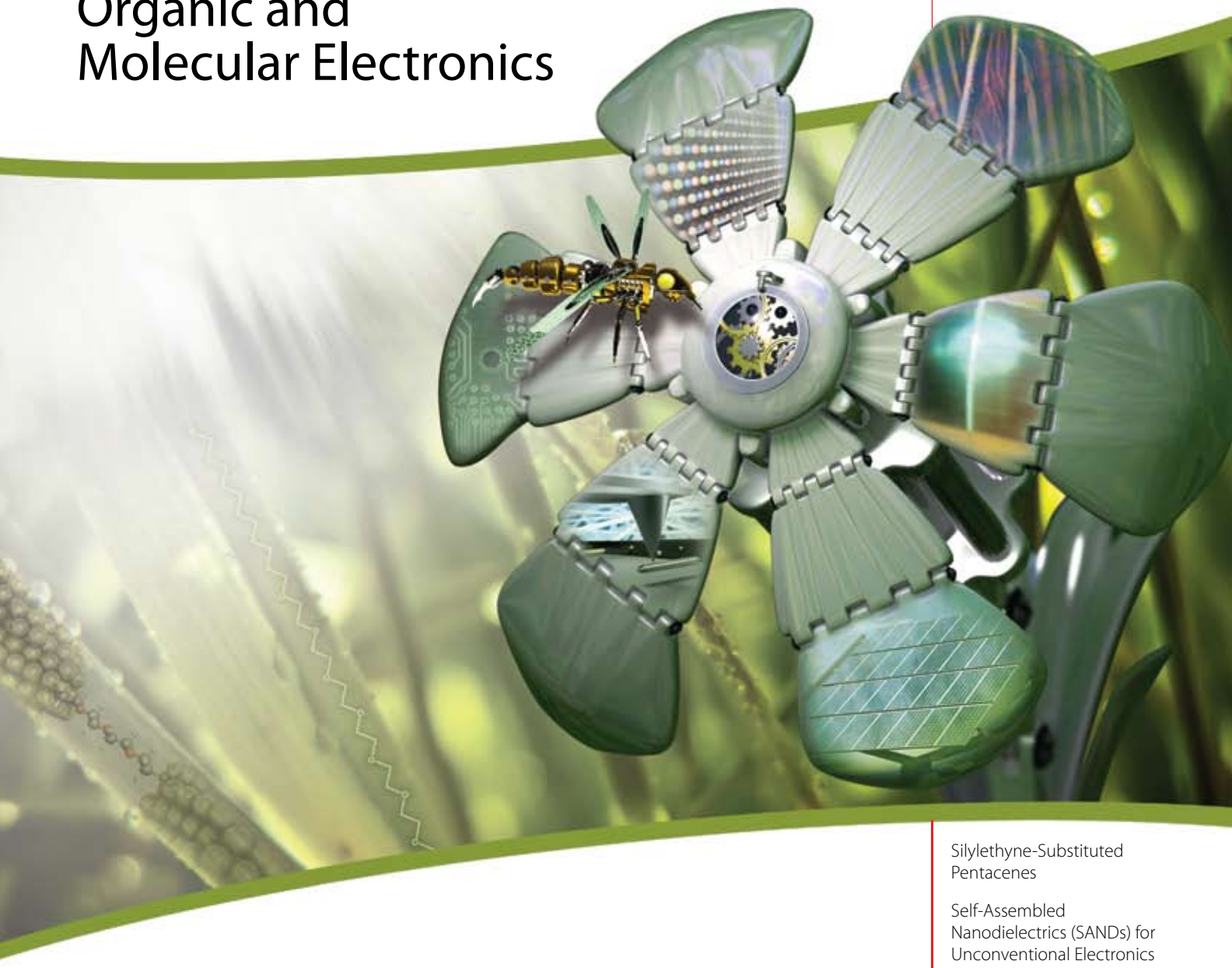

Innovation in full bloom

SIGMA-ALDRICH®

Introduction

Kaushik Patel, Ph.D.
Materials Science Initiative
Sigma-Aldrich Corporation

Welcome to the penultimate issue of ***Material Matters™*** for **2009** focused on molecular and organic electronics. Here, we display a variety of innovative technologies that, both at a fundamental level and for application, have demonstrated superior performances and capabilities.

The term 'molecular electronics' (often referred to as moletronics) is regarded as an interdisciplinary field that relies primarily on aspects of materials science, chemistry and physics. Knowledge from each of these disciplines is required when creating key molecules that can be utilized as the active (switching, sensing) or passive (current rectifiers, resistive wires) elements in electronic devices. Traditional electronics (top-down technology) has already started to approach a practical size limit. Moletronics (bottom-up strategy) has the potential to dramatically extend the miniaturization that has propelled the density and speed advantages of the integrated circuit phase per Moore's Law. The remarkable growth of molecular electronics in the last two decades is a direct reflection of the synthetic capabilities arising from surface functionalization and bonding at interfaces, in tandem with the invention/development of scanning probe technology that permits both manipulation and measurement at the nanoscale, for e.g. to make measurements in a junction containing exactly one molecule.

Research in organic electronics has witnessed similar explosive growth. The notion of creating electronic circuits and devices on plastic platforms, as apposed to a silicon foundation, provides researchers the possibility of circumventing issues such as cost, weight, widespread adoption and fragility. Global development of small molecules and polymers that are used throughout the field has accelerated, primarily in response to these advantages. The materials function as semiconductors, conductors and light emitters finding use in a myriad of applications such as smart windows, electronic paper, printed electronics inks, low-cost flexible photovoltaic devices and lasers.

This issue begins with an article by Professor John Anthony (University of Kentucky) and 3M Corporation describing the synthesis, properties and device performance of soluble TIPS (triisopropylsilyl) pentacene. The next article covers self-assembled nanodielectrics (SAND) for unconventional electronics by Professor Tobin Marks (Northwestern University) and Dr. Antonio Facchetti (Polyera Corporation). They demonstrate the genesis and performance of organic thin-film transistors (TFTs) using novel semiconductor materials and Indium Tin Oxide (ITO) substrates. Professors Iain McCulloch and Martin Heeney (Imperial College London) provide an account of organic field effect transistor devices they created using a solution processable polytriarylamine (PTAA) semiconductor. The spotlight then turns to Professor Chihaya Adachi and Dr. Hajime Nakanotani (Kyushu University) who explain the characteristics of novel organic semiconductor laser materials. These innovative materials increase efficiency of the light emitting and field effect transistors by dramatically reducing lasing thresholds. As a finale, Professor Thomas Bjørnholm (University of Copenhagen) and his team provide an elegant example of the use of self-assembly to achieve nanogaps that incorporate a single, conducting molecule, which has a well-defined contact geometry.

Aldrich Materials Science strives to be your source for the latest, most innovative products to meet and exceed your research material requirements. We are proud to offer an exciting range of materials which are discussed in the following articles. Examples include TIPS pentacene, PTAA and a large variety of gold nanostructures for your organic and molecular electronics needs.

In this issue, as in previous issues, of ***Material Matters™***, the "Your Materials Matter" section once again features a material that has been brought to our attention by a leading researcher from the scientific community. Each article in this issue is accompanied by the corresponding Aldrich Materials Science products that are the key to fabricating devices in the field of Molecular and Organic Electronics. The opposing page lists the material categories that you will find in this issue. For a comprehensive library of products and all associated information, please visit Aldrich Materials Science at *sigma-aldrich.com/matsci*. We welcome your comments and questions regarding ***Material Matters™*** or any materials of interest to matsci@sial.com.

About Our Cover

Research in Organic and Molecular Electronics requires the exploration of the nanoscale realm whether it is to understand the bulk performance of molecules in devices or to create nanogaps in which a single molecule, held between two electrodes, can be studied. Examples of devices include low-cost flexible organic solar cell devices which can harvest photons from the sun. Here we show an artist's rendition of the imagery associated with devices and materials of this field. The petals of the molecular flower are inscribed with images of organic and molecular electronics topics are described in the articles. The blue electroluminescence is from an organic lasing dye (presented in the article on page 74), in tandem with OLED devices, while the highly oriented growth of TIPS pentacene is shown in the upper right hand leaf. The molecular representation of (11-Mercaptoundecyl)hexa(ethylene glycol)monomethy ether, an adsorption-resistant self-assembly material, is shown to the left of the flower. The far left image displays an organic molecule tethered between two gold nanorods in a nanogap junction. We also cannot forget to mention our little RoboBee!

Material Matters™

Vol. 4 No. 3

Aldrich Chemical Co., Inc.
Sigma-Aldrich Corporation
6000 N. Teutonia Ave.
Milwaukee, WI 53209, USA

To Place Orders

Telephone	800-325-3010 (USA)
FAX	800-325-5052 (USA)

Customer & Technical Services

Customer Inquiries	800-325-3010
Technical Service	800-231-8327
SAFC®	800-244-1173
Custom Synthesis	800-244-1173
Flavors & Fragrances	800-227-4563
International	414-438-3850
24-Hour Emergency	414-438-3850
Web site	*sigma-aldrich.com*
Email	aldrich@sial.com

Subscriptions

To request your **FREE** subscription to *Material Matters*, please contact us by:

Phone:	**800-325-3010** (USA)
Mail:	**Attn: Marketing Communications** **Aldrich Chemical Co., Inc.** **Sigma-Aldrich Corporation** **P.O. Box 2988** **Milwaukee, WI 53201-2988**
Website:	***sigma-aldrich.com/mm***
Email:	**sams-usa@sial.com**

International customers, please contact your local Sigma-Aldrich office. For worldwide contact information, please see back cover.

Material Matters is also available in PDF format on the Internet at ***sigma-aldrich.com/matsci***.

Material Matters (ISSN 1933–9631) is a publication of Aldrich Chemical Co., Inc. Aldrich is a member of the Sigma-Aldrich Group.

"Your Materials Matter."

Joe Porwoll, President
Aldrich Chemical Co., Inc.

Do you have a compound that you wish Sigma-Aldrich® could list to help materials research? If it is needed to accelerate your research, it matters—please send your suggestion to ***matsci@sial.com*** *and we will be happy to give it careful consideration.*

Professor Koji Araki of the University of Tokyo kindly suggested that we offer 1,3,6,8-tetrabromopyrene (**Aldrich Prod. No. 717274**) as a building block for the synthesis of larger, luminescent materials. Molecules that are light emitters in the visible region are potentially useful in the fabrication of organic light emitting diodes (OLEDs).[1,2] For example, this starting material is used to create a variety of pyrene-core molecules, using high-yielding reactions such as Suzuki coupling, that can efficiently emit blue-light with efficiencies of 0.9.[3]

1,3,6,8-Tetrabromopyrene

[128-63-2] $C_{16}H_6Br_4$ FW 517.83

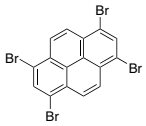

Synthetic building block for the creation of blue to green OLED emitters

717274-5G

References:

(1) a) Andrade, B. W.; Forrest, S. R. *Adv. Mater.* **2004**, *16*, 1585-1595; b) Aziz, H.; Popovic, Z. D. *Chem. Mater.* **2004**, *16*, 4522-4532.
(2) Xia, R.; Lai, W.-Y.; Levermore, P. A.; Huang, W.; Bradley, D. D. C. *Adv. Funct. Mat.* **2009**, *19*, 2844-2850.
(3) Sagara, Y.; Mutai, T.; Yoshikawa, I. ; Araki, K. *J. Am. Chem. Soc.* **2007**, *129*, 1520-1521.

Organic and Molecular Electronics Products Featured in this Issue

Silylethyne-Substituted Pentacenes

John E. Anthony*
Department of Chemistry, University of Kentucky, Lexington, KY

Dennis E. Vogel, Scott M. Schnobrich, Robert S. Clough, James C. Novack & David Redinger
Corporate Research Laboratories, 3M Center, St Paul, MN
*E-Mail: anthony@uky.edu

Introduction

Research into the use of organic semiconductors in field-effect transistors (FETs) began in earnest in the mid-1990s,[1] after early exciting results from vapor-deposited small molecule semiconductors.[2] The drive for low-cost processing capabilities then led to significant advances in polymeric semiconductors, which offered lower performance but simplified fabrication.[3] More recently, soluble small-molecule systems are providing the high performance of vapor deposited systems with the convenience of low-cost solution-based processing techniques.[4] The earliest soluble small molecule approaches involved the reversible solubilization of high-performance chromophores such as pentacene or oligothiophenes.[5] A current approach to soluble materials relies on functionalization of linearly-fused chromophores with substituents that take advantage of both steric and π-stacking interactions to induce these chromophores to self-assemble into arrays with strong intermolecular electronic coupling.[6] The resulting highly engineered materials offer simple processing from solution to yield robust electronic devices. The strong tendency for these materials to self-assemble yields uniform fields with significant long-range crystalline order, which leads to field-effect transistor devices with performance that rivals, and in some cases surpasses, the performance of vapor-deposited small molecules.

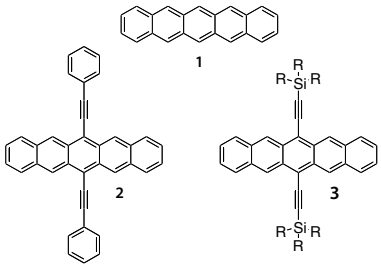

Figure 1. Pentacene (**1**), phenylethynyl pentacene (**2**) and silylethynyl pentacenes (**3**).

Of the linearly-fused compounds, pentacene (**1, Aldrich Prod. No. 698423**) is perhaps the most exhaustively studied, and is considered a "benchmark" organic semiconductor.[7] It is not surprising that this chromophore has also been the subject of numerous functionalization studies, in attempts to improve the stability and solubility of the material.[8] One of the most versatile pentacene substituent classes is the trialkylsilyl alkyne. Silylethyne substitution offers excellent opportunity to tune solubility for application-specific needs and self-assembly for electronic performance, and has yielded semiconductors with excellent device performance.

Synthesis

Ethyne-substituted pentacenes in general have been known since the 1960s, when phenylethynyl derivatives (**2**) were proposed as red emitters in chemiluminescent systems.[9] Although these materials are generally poorly soluble, recently, one phenylethyne derivative has shown reasonable mobility in top-contact devices.[10] More versatile are the trialkylsilylethynyl derivatives.[11] The synthesis of these compounds (**Scheme 1**) follows the same basic procedure as the phenylethyne derivatives, namely addition of an alkyne anion to commercially-available pentacenequinone (**4, Aldrich Prod. No. 246883**) followed by deoxygenation using either HI (**Aldrich Prod. No. 210013**) or $SnCl_2$ (**Aldrich Prod. No. 452335**).[12,13] It has recently been shown that a mixture of KI (**Aldrich Prod. No. 60399**) and NaH_2PO_2 (**Aldrich Prod. No. 58282**) in acetic acid (**Aldrich Prod. No. 338826**) is the preferred reagent in cases where the pentacene unit contains strongly electron-withdrawing groups.[14] For use in electronic devices, the purity of the resulting materials is critical - even small amounts of impurities can lead to poor film crystallinity, decreased material stability and dismal electronic performance.[15] Because of the highly non-polar nature of these molecules and the typical impurities, the separation of byproducts is often problematic. Thus, the successful synthesis relies heavily on the purity of starting materials.

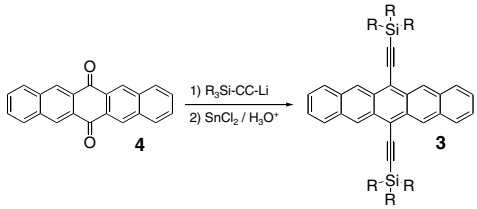

Scheme 1. Ethynylpentacene synthesis.

Crystal Packing

The formation of crystalline films of soluble pentacenes is critical, since the electronic properties of the films evolves from the crystalline arrangement of the individual molecule, and the close-packed arrangement of molecules yields significantly improved stability over amorphous films.[16] The crystal packing of silylethyne-substituted pentacenes is conveniently tuned by changing the alkyl substituents on silicon.[11] A number of examples of the crystal motifs accessible are shown in **Figure 2**. For the tert-butyldimethylsilyl (**3a**), triethylsilyl (**3b**), triisopropylsilyl (**3c**), and tris(trimethylsilyl)silyl (**3d**) derivatives shown in the **Figure 2**, we see that crystal packing can be shifted between one-dimensional columnar stacks, one-dimensional slipped stacks, two-dimensional stacks and purely edge-to-face interactions.

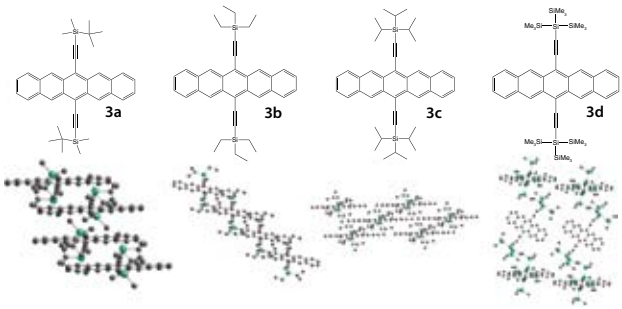

Figure 2. Representative silylethyne pentacene derivatives and their crystal packing.

Intrinsic Properties

For planar devices (such as FETs), we have found that materials with two-dimensional π-stacking interactions yield the most uniform films and provide the best device performance. Of these, the 6,13-bis(triisopropylsilylethynyl) pentacene derivative (TIPS pentacene **3c** (**Aldrich Prod. No. 716006**)) has proven to be quite successful for applications in organic electronics and is the most intensively studied soluble pentacene. Band structure calculations on a variety of silylethyne-substituted pentacenes show significant dispersion in both the conduction and valence bands, predicting significant potential for high hole and electron mobility.[17] This potential was confirmed by optical pump-THz probe studies on single crystals of TIPS pentacene **3c** and triethylsilyl derivative **3b**, showing that both materials exhibit mobilities of the same order as that of unsubstituted pentacene.[18]

OFETs

Device applications of this class of compounds were first reported in 2003, with the analysis of vapor-deposited films of a series of silylethyne-functionalized pentacenes in bottom-contact transistors.[19] A key finding of these studies was the need to heat the device substrates to over 85°C during deposition in order to achieve suitably crystalline films. Contrary to the all-optical studies performed on single crystals, the thin-film studies showed dramatic differences in performance between 1-D and 2-D π-stacked materials, with the 2-D materials (**3c**, μ_{FET} = 0.4 cm^2/Vs) vastly outperforming a variety of 1-D stacked compounds (e.g. **3b**, μ_{FET} = 10^{-5} cm^2/Vs). These differences likely arise from differences in film morphology; TIPS compound **3c** grew on the substrate as wide needles or plates, while TES derivative **3b** grew as thin needles with poor substrate coverage.[20] Subsequent studies of solution-deposited films, where the slow solvent evaporation rate allows the pentacene to self-organize during crystallization, showed significantly improved performance in FET devices based on TIPS pentacene, with hole mobility as high as 1.8 cm^2/Vs observed in films cast from toluene.[21] Careful selection of casting solvent is critical to yield high quality films and stable device performance.[22]

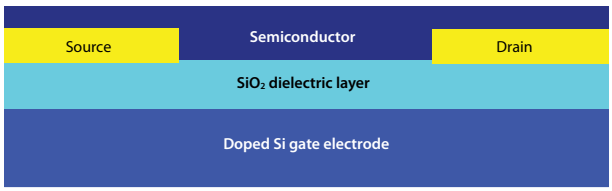

Figure 3. Bottom-contact field-effect transistor configuration, and a top-down picture of a bottom-contact device with semiconductor deposited.

Anisotropy

The highly soluble nature of the silylethyne-substituted pentacenes, coupled with their propensity to grow highly oriented crystallites on certain surfaces, allows the use of a number of process approaches to gain information on the inherent transport properties of the materials. Thin film growth on inclined substrates,[23] or under the directed flow of an inert carrier gas,[24] across source-drain electrodes arranged in a variety of orientations show that mobility can vary by an order of magnitude depending on the direction of crystal growth across the electrodes. Studies using four-electrode transistors and a hollow-pen approach to deposit ordered films observed similar anisotropy values.[25] Control of film morphology is thus critical to minimizing device-to-device performance variation in these pentacene films.

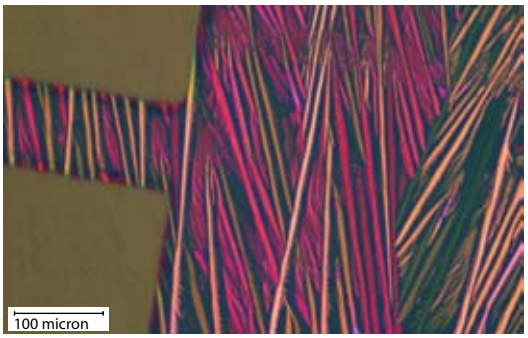

Figure 4. A device fabricated from TIPS pentacene **3c**, showing highly oriented growth of the semiconductor.

Circuits

Despite the significant anisotropy in un-oriented films of TIPS pentacene, a number of complex circuits have been demonstrated using this material. The earliest approaches used vacuum-deposited films of TIPS pentacene (typical FET mobility: 0.002-0.05 cm^2/Vs) onto pre-patterned $Si/SiO_2/Au$ substrates to yield an inverter with a gain of 5.5 at a driving voltage of -10 V.[26] They also produced functioning *NAND* and *NOR* logic gates. More recent studies using solution-deposited TIPS pentacene yielded average FET mobilities in the range of 0.2-0.6 cm^2/Vs, and produced inverters with gain of 3.5.[27] Seven-stage ring oscillators produced from these inverters yielded oscillation frequencies greater than 10 kHz, and operating voltages as low as -5 V.

Blends

To improve the film forming properties of small molecule semiconductors, the blending of molecule such as TIPS pentacene with insulating or semiconducting polymers has become a compelling strategy.[28] The polymer matrix dramatically slows the loss of solvent from the spin-cast film, allowing the small-molecule to segregate and crystallize into large grains (**Figure 5**).

Figure 5. Micrograph of a polymer/TIPS pentacene blended film formed by dip-coating. Note the morphology of the TIPS pentacene crystals is similar to that seen in non-blended films (**Figure 4**).

This approach yields the processing properties of soluble polymer materials, with the excellent electronic properties of high-performance small molecules. Recent studies of poly(α-methylstyrene)/TIPS pentacene blends showed mobility as high as 0.54 cm^2/Vs from spin-cast films.[29] Detailed analysis of these films demonstrated that the semiconductor segregated preferentially to the interface with the silica dielectric, provided that a polymer of sufficiently high molecular weight was used. Blending TIPS pentacene with poly(triarylamine) semiconducting polymers led instead to segregation of TIPS pentacene to the top (air) interface of the polymer.[30] In this case, spin-cast films in a top-gate configuration yielded saturation mobility as high as 1.1 cm^2/Vs, with good device uniformity and stability.

Inkjet Printing

Inkjet printing is emerging as a leading technology for the deposition of organic semiconductor films in a variety of organic electronic applications.[31] Early reports of printing of silylethyne-functionalized pentacenes demonstrated a need for careful selection of solvent blend, and relied on an unusual concentric ring arrangement of source and drain electrodes. With these precautions, average effective mobilities as high as 0.12 cm^2/Vs were achieved when channel width was corrected to the actual portion of the channel region covered by crystallites.[32] In late 2007, an all-inkjet-printed electrophoretic display was demonstrated using TIPS pentacene as the active transistor material.[33] By exploiting short channel length devices, mobilities over 0.01 cm^2/Vs could be achieved, allowing the fabrication of a backplane for the 10.5" 76 dpi display. We have achieved an average mobility of 0.194 cm^2/Vs for all inkjet printed TFTs (channel length = 125 µm) made with TIPS pentacene in a polystyrene blended ink using bottom gate, bottom contact devices (**Figure 6**).

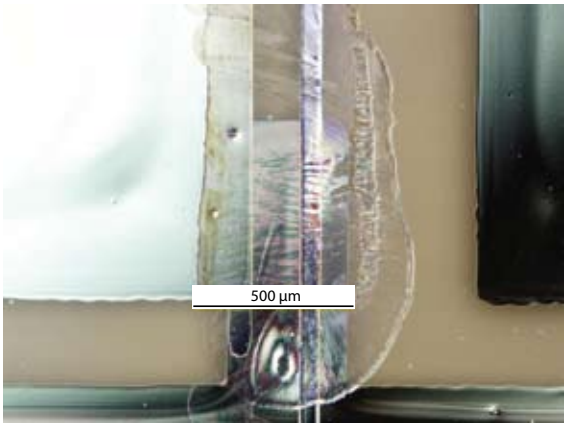

Figure 6. An inkjet printed transistor based on TIPS pentacene.

The electrodes and conductors were printed and sintered Ag nanoparticles, and the devices exhibited an on/off current ratio of 10^5, with an average threshold voltage and subthreshold slope of 0.148 V and 1.293 V/dec, respectively. An electrophoretic display driven by an all inkjet printed backplane is presented in **Figure 7**.

Figure 7. An all inkjet printed, TIPS pentacene based backplane (top) and an electrophoretic display made with that backplane (bottom).

Other Uses

TIPS pentacene has also found use as a donor in single-heterojunction solar cells (**Figure 8**). Solution deposited films of TIPS pentacene were paired with vacuum-deposited C_{60} (**Aldrich Prod. No. 572500**) as an acceptor to yield solar cells with 0.52% efficiency.[34] Alternatively, all-vacuum-deposited single heterojunction cells with TIPS pentacene and C_{60} yielded solar cells with efficiency of 0.42%.[35] Dioxole-functionalized derivative **5** performed somewhat better in these vacuum-deposited devices, yielding efficiencies up to 0.74%. Fullerene-based bulk heterojunction devices cannot be made with pentacene derivatives, due to rapid reaction between fullerenes and pentacenes.[36] Derivative **5** is an intensely fluorescent compound, and has also been used to fabricate red organic light emitting diodes with external quantum efficiency of 3.3%.[37]

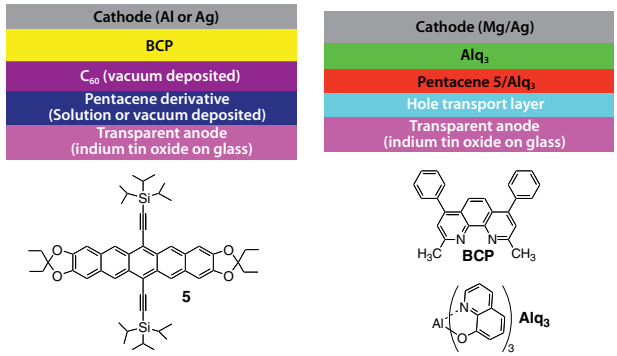

Figure 8. Top: Typical configurations for single-heterojunction organic solar cells (left) and light-emitting diodes (right). Bottom: dioxole derivative **5**.

Conclusion

Soluble semiconductors are poised to play a leading role in emerging technologies. The structural variations exemplified by silylethyne-substitute pentacene have allowed tuning of the electronic, structural and film-forming properties of the important pentacene chromophore, yielding materials for both the study of intrinsic semiconductor properties in organic materials and exploration of the devices made possible by high-performance organic semiconductors. Combined with the straightforward synthetic routes to these materials, the avenues for exploration are nearly limitless.

References:

(1) Dimitrakopoulos, C. D.; Malenfant, P. R. L. *Adv. Mater.* **2002**, *14*, 99.
(2) Murphy, A. R.; Fréchet, J. M. J. *Chem. Rev.* **2007**, *107*, 1066.
(3) Facchetti, A. *Materials Today* **2007**, *10*, 28.
(4) Mas-Torrent, M.; Rovira, C. *Chem. Soc. Rev.* **2008**, *37*, 827.
(5) For example, see Herwig, P. T.; Müllen, K. *Adv. Mater.* **1999**, *11*, 480 and Murphy, A. R.; Fréchet, J. M. J.; Chang, P.; Lee, J.; Subramanian, V. *J. Am. Chem. Soc.* **2004**, *126*, 1596.
(6) Anthony, J. E. *Chem. Rev.* **2006**, *106*, 5028.
(7) Dimitrakopoulos, C. D.; Mascaro, D. J. *IBM J. Res. Dev.* **2001**, *45*, 11.
(8) For a review of functionalized pentacene, see Anthony, J. *Angew. Chem. Int. Ed.* **2008**, *47*, 452.
(9) Mauding, D. R.; Roberts, B. G. *J. Org. Chem.* **1969**, *34*, 1734.
(10) Li, Y.; Wu, Y.; Liu, P.; Prostran, Z.; Gardner, S.; Ong, B. S. *Chem. Mater.* **2007**, *19*, 418.
(11) Anthony, J. E.; Eaton, D. L.; Parkin, S. R. *Org. Lett.* **2002**, *4*, 15.
(12) Rio, G. *Ann. Chim.* **1954**, *9*, 187.
(13) Ried, W.; Donner, W.; Schlegelmilch, W. *Ber.* **1961**, *94*, 1051.
(14) Miao, S.; Smith, M. D.; Bunz, U. H. F. *Org. Lett.* **2006**, *8*, 757.
(15) Maliakal, A.; Raghavachari, K.; Katz, H. E.; Chandross, E.; Siegrist, T. *Chem. Mater.* **2004**, *16*, 4980.
(16) Coppo, P.; Yeates, S. G. *Adv. Mater.* **2005**, *17*, 3001.
(17) Haddon, R. C.; Chi, X.; Itkis, M. E.; Anthony, J. E.; Eaton, D. L.; Siegrist, T.; Mattheus, C. C.; Palstra, T. T. M. *J. Phys. Chem. B* **2002**, *106*, 8288 and Troisi, A.; Orlandi, G.; Anthony, J. E. *Chem. Mater.* **2005**, *17*, 5024.
(18) Ostroverkhova, O.; Cooke, D. G.; Scherbyna, S.; Egerton, R. F.; Hegmann, F. A.; Tykwinski, R. R.; Anthony, J. E. *Phys. Rev. B* **2005**, *71*, 035204.
(19) Sheraw, C. D.; Jackson, T. N.; Eaton, D. L.; Anthony, J. E. *Adv. Mater.* **2003**, *15*, 2009.
(20) Ostroverkhova, O.; Shcherbyna, S.; Cooke, D. G.; Egerton, R. F.; Hegmann, F. A.; Tykwinski, R. R.; Parkin, S. R.; Anthony, J. E. *J. Appl. Phys.* **2005**, *98*, 033701.
(21) Park, S. K.; Jackson, T. N.; Anthony, J. E.; Mourey, D. A. *Appl. Phys. Lett.* **2007**, *91*, 063514.
(22) Kim, C. S.; Lee, S.; Gomez, E. D.; Anthony, J. E.; Loo, Y.-L. *Appl. Phys. Lett.* **2008**, *93*, 103302.
(23) Lee, W. H.; Lim, D. H.; Jang, Y.; Cho, J. H.; Kim, Y. H.; Han, J. I.; Cho, K. *Appl. Phys. Lett.* **2007**, *90*, 132106.
(24) Chen, J.; Tee, C. K.; Shtein, M.; Martin, D. C.; Anthony, J. *Org. Electron.* **2009**, *10*, 696.
(25) Headrick, R. L.; Wo, S.; Sansoz, F.; Anthony, J. E. *Appl. Phys. Lett.* **2008**, *92*, 063302.
(26) Park, J. G.; Vasic, R.; Brooks, J. S.; Anthony, J. E. *J. Appl. Phys.* **2006**, *100*, 044511.
(27) Park, S. K.; Anthony, J. E.; Jackson, T. N. *IEEE Electron Dev. Lett.* **2007**, *28*, 877.
(28) Hamilton, R.; Smith, J.; Ogier, S.; Heeney, M; Anthony, J. E; McCulloch, I.; Veres, J.; Bradley, D. D. C.; Anthopoulos, T. D. *Adv. Mater.* 2009, 21, 1166.
(29) Kang, J.; Shin, N.; Jang, D. Y.; Prabhu, V. M.; Yoon, D. Y. *J. Am. Chem. Soc.* **2008**, *130*, 12273 and Ohe, T.; Kuribayashi, M.; Yasuda, R.; Tsuboi, A.; Nomoto, K.; Satori, K.; Itabashi, M.; Kasahara, J. *Appl. Phys. Lett.* **2008**, *93*, 053303.
(30) Hamilton, R.; Smith, J.; Ogier, S.; Heeney, M.; Anthony, J. E.; McCulloch, I.; Veres, J.; Bradley, D. D. C.; Anthopoulos, T. D. *Adv. Mater.* **2009**, *21*, 1166.
(31) *Printed Organic and Molecular Electronics* (Eds. : D. Gamota, P. Brazis, K. Kalyanasundaram, J. Zhang), Springer, Berlin, **2005**.
(32) Lim, J. A.; Lee, W. H.; Lee, H. S.; Lee, J. H.; Park, Y. D.; Cho, K. *Adv. Func. Mater.* **2008**, *18*, 229.
(33) Okubo, T.; Kokubo, Y.; Hatta, K.; Matsubara, R.; Ishizaki, M.; Ugajin, Y.; Sekine, N.; Kawashima, N.; Fukuda, T.; Nomoto, A.; Ohe, T.; Kobayashi, N.; Nomoto, K.; Kasahara, J. Proceedings of the 14th International Display Workshop (IDW '07) **2007**, *2*, AMD5-4L, 463.
(34) Lloyd, M. T.; Mayer, A. C.; Tayi, A. S.; Bowen, A. M.; Kasen, T. G.; Herman, D. J.; Mourey, D. A.; Anthony, J. E.; Malliaras, G. G. *Org. Electron.* **2006**, *7*, 243.
(35) Pallilis, L. C.; Lane, P. A.; Kushto, G. P.; Purushothaman, B.; Anthony, J. E.; Kafafi, Z. H. *Org. Electron.* **2008**, *9*, 747.
(36) Miller, G. P.; Briggs, J.; Mack, J.; Lord, P. A.; Olmstead, M. M.; Balch, A. L. *Org. Lett.* **2003**, *5*, 4199. (37) Wolak, M. A.; Delcamp, J.; Landis, C. A.; Lane, P. A.; Anthony, J.; Kafafi, Z. *Adv. Func. Mater.* **2006**, *16*, 1943.

Pentacenes

For sublimed grade materials, see page 77.

Name	Structure	Solubility	Cat. No.
6,13-Bis(triisopropylsilylethynyl) pentacene	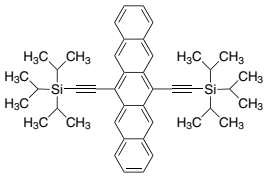	organic solvents, soluble, (lit)	716006-250MG 716006-1G
Pentacene, ≥99.995% trace metals basis	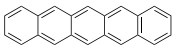	organic solvents, low solubility, (lit)	698423-500MG
Pentacene, ≥99.9% trace metals basis		organic solvents, low solubility, (lit)	684848-1G
Pentacene		organic solvents, low solubility, (lit)	P1802-100MG P1802-1G P1802-5G

TIPS Pentacene is a product of 3M.

Soluble Pentacene Precursors

Name	Structure	Solubility	Cat. No.
Pentacene-*N*-sulfinyl-*tert*-butylcarbamate, 99% (HPLC)	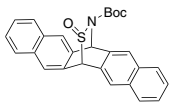	ethanol 1 mg/mL, slightly soluble tetrahydrofuran 1 mg/mL, soluble methanol 1 mg/mL, slightly soluble isopropanol 1 mg/mL, slightly soluble	699306-100MG 699306-500MG
13,6-*N*-Sulfinylacetamidopentacene, 97%	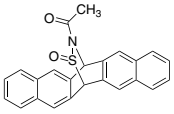	dioxane, soluble methylene chloride, soluble tetrahydrofuran, soluble	666025-100MG 666025-500MG
6,13-Dihydro-6,13-methanopentacene-15-one, 97%	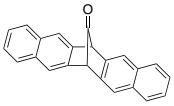	chloroform ~0.7 mg/mL, slightly soluble toluene ~0.7 mg/mL, slightly soluble	688045-100MG 688045-500MG

Fullerene Materials

For a complete list of fullerenes, please visit ***sigma-aldrich.com/nanocarbon***

PCBM & Small Gap Fullerene Analogs

Name	Structure	Solubility	Cat. No.
Small gap fullerenes, ≥98%*	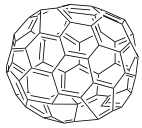	organic solvents, soluble	707503-1G
Polyhydroxy small gap fullerenes, hydrated*	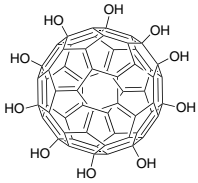	water, pH>9, soluble	707481-100MG
Small gap fullerene-ethyl nipecotate*	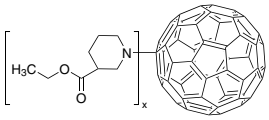	organic solvents, soluble toluene, soluble	707473-250MG
C_{60} Pyrrolidine tris-acid	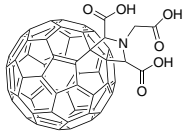	water, pH>9, soluble	709085-100MG
C_{60} Pyrrolidine tris-acid ethyl ester, 97% (HPLC)	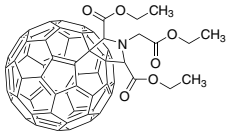	chlorobenzene, soluble toluene, soluble organic solvents, soluble	709093-250MG
[6,6]-Phenyl C_{61} butyric acid methyl ester, >99.9%	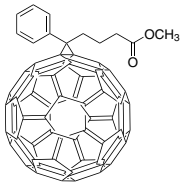	chlorobenzene, soluble toluene, soluble organic solvents, soluble	684457-100MG
[6,6]-Phenyl C_{61} butyric acid methyl ester, >99%		chlorobenzene, soluble toluene, soluble organic solvents, soluble	684430-1G
[6,6]-Phenyl C_{71} butyric acid methyl ester, mixture of isomers, 99%	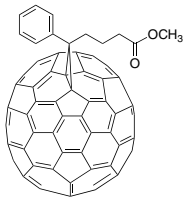	chlorobenzene, soluble organic solvents, soluble toluene, soluble	684465-100MG 684465-500MG

*Product of TDA Research, Inc. and US Patents 6,517,799, 6,303,016, 6,517,799

Name	Structure	Solubility	Cat. No.
[6,6]-Phenyl C_{85} butyric acid methyl ester, mixture of isomers, ≥99%	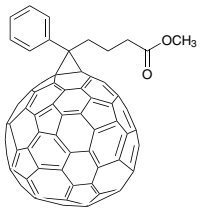	chlorobenzene, soluble organic solvents, soluble toluene, soluble	684473-100MG
[6,6]-Thienyl C_{61} butyric acid methyl ester, ≥99%	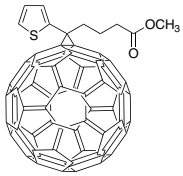	organic solvents, soluble	688215-100MG
[6.6] Diphenyl C_{62} bis(butyric acid methyl ester)(mixture of isomers), 99.5%	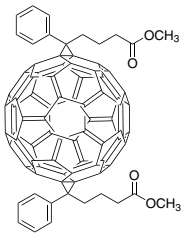	organic solvents, soluble	704326-100MG

Additional Fullerenes

Name	Structure	Solubility	Cat. No.
Fullerene-C_{60}, 99.9%	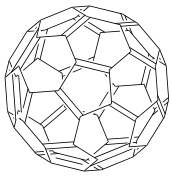	organic solvents, soluble	572500-250MG 572500-1G
Fullerene-C_{60}, 99.5%		organic solvents, soluble	379646-100MG 379646-1G 379646-5G
Fullerene-C_{60}, 98%		organic solvents, soluble	483036-1G 483036-5G
[5,6]-Fullerene-C_{70}, sublimed grade	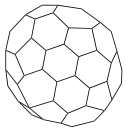	toluene, soluble benzene, soluble	709476-250MG
[5,6]-Fullerene-C_{70}, 99%		toluene, soluble benzene, soluble	482994-100MG 482994-500MG
Fullerene-C_{76}, 98%	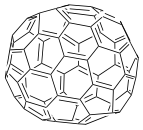	organic solvents, soluble	482951-5MG
Fullerene-C_{84}, 98%	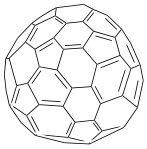	organic solvents, soluble	482986-5MG

Self-Assembled Nanodielectrics (SANDs) for Unconventional Electronics


Antonio Facchetti
Polyera Corporation, www.polyera.com
E-mail: afacchetti@polyera.com

Tobin J. Marks
Department of Chemistry, Northwestern University, Evanston, IL
E-mail: t-marks@northwestern.edu

Introduction

The field of unconventional electronics represents a new opportunity for the semiconductor and electronics industries.[1] This broad field encompasses both "printed organic/inorganic" and "transparent" electronics. The first technology aims at the fabrication of extremely cheap electronic devices such rf-id tags, 'smart' cards, flexible electronic paper, and backplane circuitry for active matrix displays by high throughput manufacturing, while the second targets "invisible" devices such as transparent circuits and monitors. The key component of all modern electronics is the thin-film transistor (TFT, See **Figure 1** for structure and function). The three fundamental TFT materials components are the contacts (source, drain, and gate), the semiconductor, and the gate dielectric.

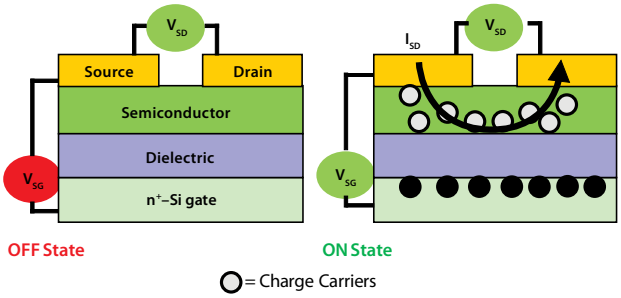

Figure 1. Structure and operation of a thin-film transistor. The basic equation describing the TFT drain current in saturation is $I_{SD} = (W/2L)\ \mu C_i\ (V_{SG}-V_T)^2$ (**eq. 1**), where μ is the field-effect carrier mobility of the semiconductor, W the channel width, L the channel length, C_i the capacitance per unit area of the dielectric layer, V_T the threshold voltage, V_{SD} the drain voltage, and V_G the gate voltage. In contrast to conventional Si transistors, organic TFTs normally operate in the accumulation mode, where applying a gate voltage creates mobile charge carriers in the channel, thus switching the device "on". The semiconductor field-effect mobility is calculated from the I-V data according to **eq. 1**. The device current I_{on}:I_{off} ratio, and the subthreshold slope (related to how efficiently the gate field modulates the off to on current and how crisply the device turns on) are also important TFT performance characteristics.

While much of the attention has been focused on the search for high-mobility, stable, and possibly printable/transparent semiconductors, it is now clear that the use of a proper gate dielectric is necessary to optimize device performance. Self-assembled nanodielectrics (SANDs) are gaining significant attention as gate dielectrics due to their robust insulating properties, tunable thicknesses at the nanometer level, optical transparency in the visible range, and efficient solution processability. In this article, we survey basic SAND structure, function, and implementation with a variety of semiconductors for TFT fabrication.[2]

SAND Chemistry, Fabrication, and Properties

Traditionally, organic/transparent TFTs have been fabricated using a 100-300 nm thick SiO_2 (**Aldrich Prod. No. 637246**) insulating layer as the gate dielectric.[3] This material prevents current leakage between the source/drain contacts and the gate, and allows accurate electrical performance characterization of the semiconducting layer. A major motivation to search for alternative gate dielectrics is to enable inexpensive TFT fabrication and to significantly reduce the operating voltages. Lower operating voltages mean lower power consumption and batteries more compatible with portable electronics. According to equation 1 (**Figure 1** caption), a viable approach to substantially increase TFT source-drain current (I_{SD}) while operating at low biases is to increase the capacitance of the gate dielectric, $C_i = \varepsilon_0(k/d)$, where k is the dielectric constant of the material, and d the insulator thickness. Importantly, alternative TFT gate dielectrics such as SAND must not only have large capacitance but also exhibit acceptable (<1% of the I_{SD}) gate leakage currents. SAND dielectrics are a type of self-assembled multilayers, which are composed of ordered molecular assemblies formed by the spontaneous adsorption of active molecular precursor(s) onto solid surfaces. Usually the precursor molecular species are sequentially deposited from common organic solvents. In the case of SAND fabrication, organosilane molecules (**Alk**, **Stb**, and **Cap**, see **Figure 2**) are employed. This self-assembly chemistry requires hydroxylated substrate surfaces, such as those of the technologically relevant SiO_2, Al_2O_3, (**Aldrich Prod. No. 642991**) and indium tin doped oxide (ITO) (**Aldrich Prod. No. 544876**) surfaces. The driving force for self-assembly is in the in situ formation of siloxane linkages, which connects the precursor silane to the surface hydroxyl (-OH) groups via strong covalent -Si-O- bonds. The present method for SAND fabrication involves iterative application of (**Figure 2**): (a) *Self-assembled α,ω-difunctionalized hydrocarbon chains* $[Cl_3Si(CH_2)_nSiCl_3]$ (**Alk**). Difunctional hydrocarbon monolayers undergo transverse crosslinking, enabling precision, stepwise layer build-up, increasing interchain packing and reducing defects/pinholes. (b) *Highly polarizable "push-pull" stilbazolium layers* (**Stb**). Self-assembled, oriented π-electron dipolar layers stabilize charge carriers in the proximate semiconducting channel when the device is turned on ($V_G \neq 0$). (c) *Octachlorotrisiloxane capping layers* (**Cap**). Multilayer structural robustness can be further enhanced by capping/planarizing with a highly crosslinked, glassy siloxane polymer.

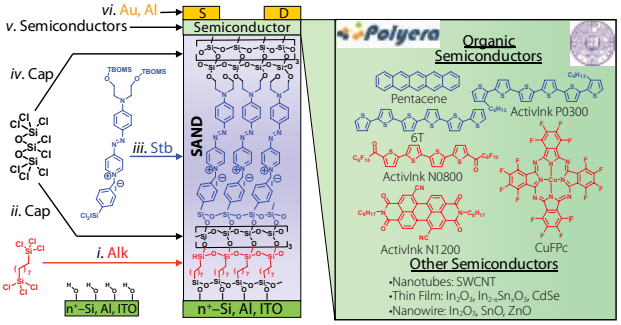

Figure 2. Left: Schematic representation of the components of a thin-film transistor (TFT) with the indicated the self-assembled nanodielectric (SAND) structure of Type III (right) on highly doped Si(100), Al, or ITO substrates/gate electrodes. Nanodielectric layers (5.5 nm thick for Type III SAND) are then sequentially deposited from solutions via layer-by-layer deposition of silane precursors **Alk**, **Stb**, or **Cap** (left), following the procedure from step ***i.*** to ***iv.*** The OTFT device is completed by deposition of the semiconductor (step ***v***) and finally by the source-drain electrodes (step ***vi***). Right: Chemical structure of some p- (blue) and n-type (red) organic semiconductors used with SANDs (some of them are commercially available at www.polyera.com) as well as a selection of other semiconductors employed to fabricate SAND-based TFTs.

Different types of SAND multilayer structures can be obtained (and were studied) by various layer percursor combinations. The most common SANDs are identified by the following nomenclature: **Alk**+**Cap** layers (Type **I**), **Stb**+**Cap** layers (Type **II**), and **Alk**+**Cap**+**Stb**+**Cap** layers(Type **III**). The most used SAND for the fabrication of TFTs with organic semiconductors is Type **III** (~5.5 nm thick) whereas for inorganic semiconductor-based TFTs, the one used most is a trilayer of Type **III** (Type **IIIx3**, ~16 nm thick). The microstructures and electrical properties of SANDs have been characterized by x-ray reflectivity, optical absorption spectroscopy, optical second-harmonic generation measurements, atomic force microscopy, and scanning electron microscopy. SANDs were established as excellent, pinhole-free insulators via solution-phase cyclic voltammetry and MIS leakage current measurements (current densities ~10^{-8}-10^{-5} A/cm^2), and measured breakdown fields were ~5-7 MVcm^{-1}. Capacitance-voltage (*C-V*) measurements on MIS structures reveal maximum capacitances C_i = 400 (**I**); 710 (**II**); 390 (**III**), ~180 (Type **IIIx3**) nFcm^{-2} at 10^2 Hz (**Figure 3**) vs. ~11 nFcm^{-2} for 300 nm-thick SiO_2.

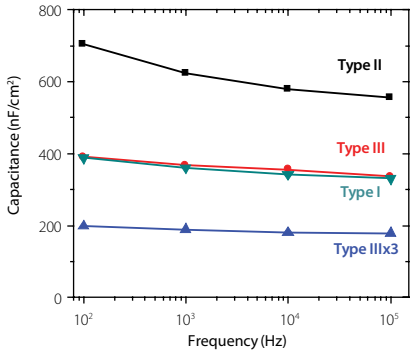

Figure 3. Frequency (*f*) dependence of the capacitance in the accumulation regime (1.0 V) between 10^2 - 10^5 Hz for the indicated SAND nanodielectrics.

Thus, considerable TFT driving voltage reduction is possible (vide infra). Recently, it was found that the annealing of **I**-**III** at 120-180°C reduces *C-V* hysteresis and frequency-dependent *C-V* dispersion. SAND Type **IIIx3** films are also exceptionally thermally stable, and the annealing of these films at 400°C enhances dielectric strength, reduces current leakage, and increases capacitance, thus opening unprecedented opportunities for integration with high-temperature processed inorganic semiconductors.

Organic Semiconductor-SAND Transistors

First-generation SAND-based organic TFTs were fabricated on doped silicon substrates (gates) using a variety of organic semiconductors discovered/developed at Northwestern University and Polyera Corporation.[5,6] In initial studies, the semiconductor layer was deposited by vapor deposition or spin-coating, and the device structure was completed by Au source/drain deposition. However, recent work at Polyera demonstrates that inkjet printing of the semiconductor on SANDs is possible. The investigated semiconductors include various pentacenes, oligothiophenes, polythiophenes, metallophthalocyanines, and perylenes. All SAND-organic semiconductor-based devices exhibit reproducible I-V characteristics at very low biases with classical linear and saturation response properties, as exemplified by data for typical p-type (hole conductor; Polyera ActivInk P0300) and n-type (electron conductor; Polyera ActivInk N1200) organic semiconductors (**Figure 4**).

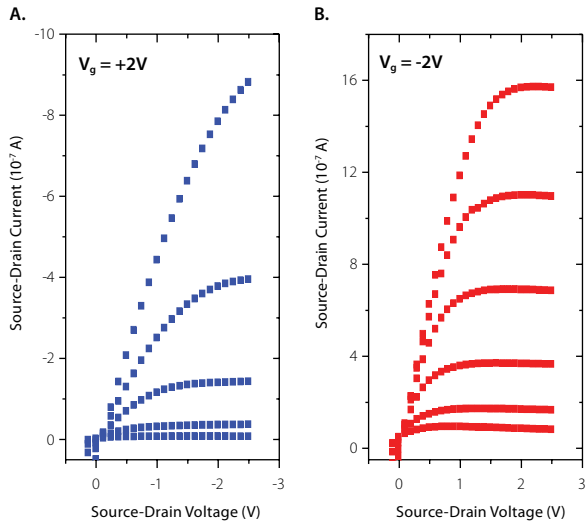

Figure 4. Performance output characteristics as a function of gate voltage (V_G) for SAND-based organic transistors with p-channel (ActivInk P0300) and n-channel (ActivInk N1200) organic semiconductors.

In marked contrast to these results, control devices fabricated with the commonly used SiO_2 dielectric (300 nm thick, C_i ~11 nF/cm^2) exhibit no useful source-drain current modulation over these same voltage ranges. Carrier mobilities for these semiconductors are similar to those obtained on Si-SiO_2 substrates, ~0.1 cm^2/Vs for both ActivInk P0300 and ActivInk N1200. Note that also TFTs fabricated on ITO-coated glass gates function comparably, demonstrating that a Si/SiO_2 native oxide gate electrode is not required to achieve excellent dielectric performance. Finally, these nanodielectrics can be used to fabricate flexible TFTs on commercially-available ITO-coated plastic (Mylar) gates, demonstrating applicability to flexible plastic electronics.

Inorganic Semiconductor-SAND Transistors and Circuits

We next investigated SAND compatibility with semiconductors other than small organic molecules. We first demonstrated the compatibility of Type **IIIx3** SAND with single-wall carbon nanotubes (SWCNTs) (**Aldrich Prod. No. 704113, 704121, 704148**) as the semiconductor.[7] SWCNTs where grown by CVD onto SiO_2/Si wafers and transfer printed (~10 tubes/μm^2) directly onto the Si-SAND substrates (and control Si/SiO_2 substrates). Good SWNT-SAND adhesion allows direct photolithographic patterning of the source and drain electrodes by liftoff. It is found that TFT performance is significantly improved over control devices using 100 nm Si/SiO_2 gate dielectrics, with substantially lowered hysteresis and V_T shifts. Thus, the TFT mobility is excellent with μ_{hole} ~5.6 cm^2/Vs, V_T = 0.2 V, and a low gate leakage current of ~10 nA at V_G = -1 V demonstrated. Furthermore, compatibility with n-type SWCNTs (those having a PEI coating) is demonstrated, with small observed hysteresis and TFT properties: $\mu_{electron}$ = 4.1 cm^2/Vs and V_T = -2 V. Compatibility of SAND dielectrics with thin-film inorganic semiconductors was demonstrated by using In_2O_3 thin-films (**Aldrich Prod. No. 203424**) to enable high-performance, low-voltage, and fully transparent TFTs.[8] In_2O_3 is a wide-bandgap (3.6-3.75 eV) n-type semiconductor with excellent transparency in the visible region (>90%). Thin films of In_2O_3 were deposited at room temperature by ion-assisted deposition (IAD) directly on top of the SAND dielectric, and device fabrication completed by Au source/drain contact deposition. Note that the SAND is stable to the in-situ ion/plasma exposure during In_2O_3 deposition. Significant In_2O_3 TFT performance enhancement is observed with SAND-gated devices, where μ = 140 cm^2/Vs, interfacial trap density, $D = 10^{11}$ cm^{-2}, V_T = 0.0 V (with nearly hysteretic free response), on/off = 10^5, and the subthreshold slope = 150 mV/decade. These metrics can be compared to the performance on Si/SiO_2-gated devices where μ = 10 cm^2/Vs and on/off = 10^5. To realize fully transparent TFTs, the same fabrication procedures were followed except utilizing glass/ITO as the bottom gate electrode and doped In_2O_3 source and drain electrodes. The performance of SAND-based transparent TFTs is essentially the same as on n$^+$-Si substrates but with an improved subthreshold slope = 90 mV/decade.

The versatility of SAND as an effective gate dielectric for non-organic semiconductors was further demonstrated in TFTs using ZnO, In_2O_3, and SnO nanowires (NWs).[9] As an example, ZnO NW (nanowire) TFTs with SAND **IIIx3** as the gate dielectric were fabricated with ZnO nanowires (80 nm average diameter, and 5 μm average length) dispersed in 2-propanol (**Aldrich Prod. No. 278475**) and then transferred to the SAND-coated Si substrates. Source and drain Al electrodes were deposited by electron beam evaporation and patterned by photolithography. The SAND dielectrics were first electrically characterized in MIS devices (Al/SAND/Si), where a leakage current density of ~10^{-8} A/cm^2 was measured, verifying SAND compatibility with the photolithographic and e-beam evaporation methodologies. SAND gated ZnO_2 NW-TFTs reduced operating voltages to <1.5 V (from >1.5 V on Si/SiO_2), while maintaining the device on/off ratio, increasing the on-current to 2 μA (from 0.3 μA), and increasing the mobility and transconductance. The V_T of SAND gated ZnO NW-TFTs is -0.4 V, and the subthreshold slope is 400 mV/decade. High subthreshold slopes usually indicate surface traps, so the SAND-based ZnO NW-TFTs were then treated with ozone exposures, and indeed the subthreshold slope was reduced to 150 mV/decade. In addition, reduced V_T values (0.2 V) and improved on:off ratios (10^8) were observed. The calculated electron mobility (taking into account the cylindrical geometry of the channel) is 196 cm^2/Vs, which is far greater than 8-18 cm^2/Vs measured for ZnO NW on thick Si/SiO_2 dielectrics, and 54 cm^2/Vs for a 70 nm thick SiO_2 control dielectric. The TFT mobility varies from 164-181 cm^2/Vs with variations in NW diameter and length. One of the remarkable properties of SAND-based electronics is their resistance to radiation damage, known as radiation hardness. The proton (10 MeV H$^+$) radiation tolerance was investigated first for SAND **IIIx3**/ZnO-NW TFTs.[10] After various dosing and exposure conditions in a nuclear reactor, neither the leakage current nor the V_T of the SAND-gated TFTs shifts significantly. Currently SAND-gated organic and inorganic TFTs are on the International Space Station for additional radiation testing. These results suggested that the bulk oxide trap density and interface trap density formed in SAND (or at the SAND-ZnO NW interface) during H$^+$ irradiation are significantly lower than in traditional SiO_2 gate dielectrics. This prompted detailed studies of ZnO-NW TFTs using low-frequency noise and temperature-dependent *I-V* measurements to characterize the surface/interface states. Lower 1/f noise constants are found for SAND-based devices compared to SiO_2-based devices, and it is concluded that the interface trap densities are comparable to those for the aforementioned SWCNT devices (D = ~10^{12} cm^{2}V^{-1}) by comparison of the Hooge's constant metric. Larger temperature variations of the transfer curves, and larger threshold voltage shifts vs. temperature observed for SiO_2/ZnO-NW TFTs versus the corresponding SAND-gated devices, provide further evidence that the SAND/ZnO-NW TFTs have exceptionally low interface trap and defect densities.

All of the processes described above demonstrate that SANDs are robust gate dielectrics compatible with a number of inorganic semiconductors. However, since the above semiconductor depositions were all carried out near room temperature, the question arises as to whether SAND is stable at higher temperatures. Very recently we demonstrated that SAND **IIIx3** films are stable to 400°C, thus opening a broad range of processing possibilities at high temperatures.[11] One particular challenge has been to implement organic dielectric materials with aqueous solution-processed inorganic semiconductors. To achieve this, we explored the compatibility of SAND-based TFTs with solution-processed cadmium selenide (CdSe) (**Aldrich Prod. No. 244600**), In_2O_3, and ITO as the semiconducting layers. As an example, the chemical bath deposition method was recently used to deposit the CdSe films on SAND **IIIx3** gate dielectric layers. Optimum performance of on:off ratio = 10^6, V_T = 3.0 V, and subthreshold slope = 0.26 V/decade was achieved for CdSe/SAND-based TFTs annealed at 400°C, which exhibit mobilities of ~40 cm^2/Vs vs. ~4 cm^2/Vs for the analogous SiO_2-based devices. Excellent performance was also achieved with In_2O_3[12] and ITO as the TFT semiconductors.

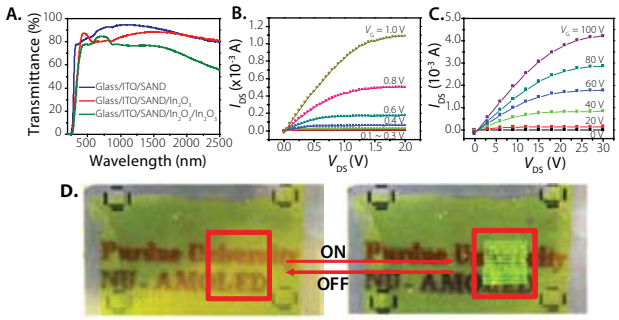

Figure 5. A. Optical transmittance of multilayer films used to fabricate transparent TFTs based on SAND gate dielectrics and a thin film of In_2O_3. **B, C.** Output transistor characteristics of IAD In_2O_3 thin film with SAND (B) and SiO_2 (C). Note the difference in the operating voltages. **D.** Partially transparent active-matrix organic LED display based on nanowire electronics.

Finally, we demonstrated the application of SAND/nanowire technology to realize fully transparent circuitry based on ZnO and In_2O_3 nanowires and ITO or AZO (Al-Zn-O) source/drain/gate contacts.[13] From this starting point, active matrix organic light-emitting diode (AMOLED) displays were fabricated with switching and driving circuits comprised exclusively of nanowire transistor (NWT) electronics fabricated at room temperature (**Figure 5**). The mobilities of these SAND-based In_2O_3

NW TFTs are ~160 cm^2/Vs, sufficient to drive bright display pixels. Fully transparent, proof-of-concept 2 x 2 mm NW-AMOLED arrays (300 pixels = 900 NWTs) were fabricated using very thin Al cathodes on glass substrates.[12] The optical transmission values are ~72% (before OLED deposition) and ~35% (after OLED deposition; thinner Al is required) in the 350-1350 nm wavelength range, which corresponds to a green peak luminescence of >300 cd/m^2. Note that transmission coefficients up to 70% have been reported for OLED structures on plastic substrates, although values in the 50% range are more common.

Conclusions

In this short account, we briefly summarized the potential and promise of self-assembled multilayer gate dielectric films fabricated from silane precursors for organic, inorganic, and transparent TFTs, as well as for TFT circuitry and OLED displays. These materials beautifully illustrate the potential of molecular chemistry for constructing unusual and useful electronic materials.

Acknowledgments

We thank ONR (N00014-05-1-0766), AFOSR (FA9550-08-1-0331), and Polyera Corp. for support of this research, and the NSF-MRSEC program through the Northwestern University Materials Research Science and Engineering Center (DMR-0520513) for providing both support and characterization facilities. We thank all of our collaborators for the important and enthusiastic contributions to this work.

References:

(1) (a) Sun, Y.; Rogers, J. A. *Adv. Mater.* **2007**, *19*, 1897. (b) Nomura, K.; Ohta, H.; Takagi, A.; Kamiya, T.; Hirano, M.; Hosono, H. *Nature* **2004**, *432* , 488. (c) Sun, B.; Peterson, R. L.; Sirringhaus, H.; Mori, K. *J. Phys. Chem. C* **2008**, *111*, 18831. (d) Murphy, A. R.; Frechet, J. M. J. *Chem. Rev.* **2007**, *107*, 1066. (e) Locklin, J.; Roberts, M.; Mannsfeld, S.; Bao, Z. *Polym. Rev.* **2006**, *46*, 79. (f) Anthopoulos, T. D.; Setayesh, S.; Smits, E.; Colle, M.; Cantatore, E.; de Boer, B.; Blom, P. W. M.; de Leeuw, D. M. *Adv. Mat.* **2006**, *18*, 1900. (g) Chabinyc, M.; Loo, Y. L. *J. Macromol. Sci. Polym. Rev.* **2006**, *46*, 1. (h) Muccini, M *Nature Mater.* **2006**, *5*, 605. (i) Chua, L.-L.; Zaumseil, J.; Chang, J.-F.; Ou, E. C.-W.; Ho, P. K.-H.; Sirringhaus, H.; Friend, R. H. *Nature* **2005**, *434*, 194.

(2) DiBenedetto, S. A.; Facchetti, A.; Ratner, M. A.; Marks, T. J. *Adv. Mater.* **2009**, *21*, 1407.

(3) Facchetti, A.; Yoon, M.-H.; Marks, T. J. *Adv. Mater*, **2005**, *17*, 1705.

(4) Yoon, M.-H.; Facchetti, A.; Marks, T.J. *Proc. Nat. Acad. Sci. USA*, **2005**, *102*, 4678.

(5) Facchetti, A.; Deng, Y.; Wang, A.; Koide, Y.; Sirringhaus, H.; Marks, T. J.; Friend, R. H. *Angew. Chem., Int. Ed.* **2000**, *39*, 4547.

(6) Jones, B. A.; Ahrens, M. J.; Yoon, M.-H.; Facchetti, A.; Marks, T. J.; Wasielewski M. R. *Angew. Chem. Int. Ed.* **2004**, *43*, 6363.

(7) Hur, S.-H.; Yoon, M.-H.; Gaur, A.; Facchetti, A.; Marks, T. J.; Rogers, J. A. *J. Am. Chem. Soc.* **2005**, *127*, 13808.

(8) Wang, L.; Yoon, M-H.; Lu. G.; Yang, Y.; Facchetti, A.; Marks, T. J. *Nature Mater.* **2006**, *5*, 893.

(9) Ju, S.; Ishikawa, F.; Chen, P.; Chang, H.-K.; Zhou, C.; Ha, Y.-G.; Liu, J.; Facchetti, A.; Marks, T. J.; Janes, D. B. *Appl. Phys. Lett.* **2008**, *92*, 222105/1.

(10) Ju, S.; Lee, K.; Janes, D. B.; Dwivedi, R. C.; Baffour-Awuah, H.; Wilkins, R.; Yoon, M.-H.; Facchetti, A. ; Marks, T. J. *Appl. Phys. Lett.* **2006**, *89*, 073510.

(11) Byrne, P.; Facchetti, A.; Marks, T. J. *Adv. Mater.* **2008**, *20*(12), 2319.

(12) Kim, H.S.; Byrne, P.D.; Facchetti, A.; Marks, T.J. *J. Am. Chem. Soc.*, **2008**, *130*, 12580.

(13) Ju, S.; Li, J.; Liu, J.; Chen, P.-C.; Ha, Y.-G.; Ishikawa, F.; Chang, H.; Zhou, C.; Facchetti, A. ; Janes, D. B.; Marks, T. J. *Nano Letters* **2008**, *8*(4), 997.

Molecular Semiconductors

Sigma-Aldrich offers many small molecule semiconductors for applications in organic electronics. The following tables list a selection of the available n-type and p-type materials. For a complete list, please visit ***sigma-aldrich.com/semiconductors***

n-Type Semiconductors

Name	Structure	Mobility	Cat. No.
7,7,8,8-Tetracyanoquinodimethane (TCNQ), 98%	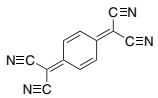	10^{-5} $cm^2/V{\cdot}s$	157635-5G 157635-10G
2,3,5,6-Tetrafluoro-7,7,8,8-tetracyanoquinodimethane (F4TCNQ), 97%	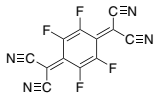	-	376779-25MG 376779-100MG
1,4,5,8-Naphthalenetetracarboxylic dianhydride (NTCDA)	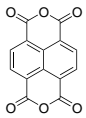	0.003 $cm^2/V{\cdot}s$	N818-5G N818-25G N818-100G
Perylene-3,4,9,10-tetracarboxylic dianhydride (PTCDA), 97%	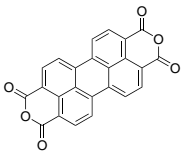	10^{-4} $cm^2/V{\cdot}s$	P11255-25G P11255-100G
N,N'-Dipentyl-3,4,9,10-perylenedicarboximide (PTCDI-C5), 98%	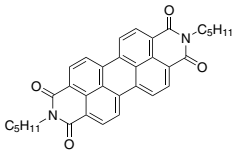	~10^{-2} $cm^2/V{\cdot}s$	663921-500MG

Name	Structure	Mobility	Cat. No.
N,N'-Dioctyl-3,4,9,10-perylenedicarboximide (PTCDI-C8), 98%	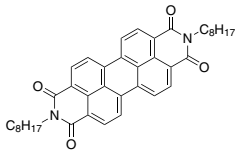	1.7 $cm^2/V{\cdot}s$	663913-1G
N,N'-Diphenyl-3,4,9,10-perylenedicarboximide (PTCDI-Ph), 98%	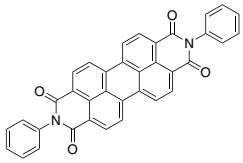	10^{-5} $cm^2/V{\cdot}s$	663905-500MG
5,10,15,20-Tetrakis(pentafluorophenyl)-21*H*,23*H*-porphine palladium(II)	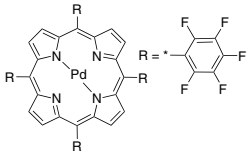	-	673587-100MG
Copper(II) 1,2,3,4,8,9,10,11,15,16,17,18,22,23,24,25-hexadecafluoro-29*H*,31*H*-phthalocyanine ($F_{16}CuPc$)	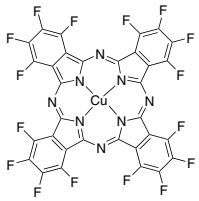	-	446653-1G

*Literature values for carrier mobility from: Shirota, Y; Kageyama, H. *Chem. Rev.* **2007**, *107*, 953; Murphy, A. R.; Fréchet, J. M. J. *ibid.* 1066.

p-Type Semiconductors

Name	Structure	Cat. No.
2,2':5',2"-Terthiophene, 99%	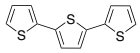	311073-1G
α-Sexithiophene (6T)	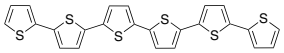	594687-1G
3,3'''-Dihexyl-2,2':5',2":5",2'''-quaterthiophene (DH-4T), 95%	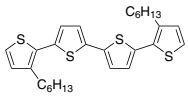	694460-1G
3,3'''-Didodecyl-2,2':5',2":5",2'''–quaterthiophene, 97%	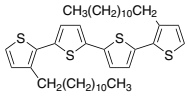	691631-500MG
Dibenzotetrathiafulvalene (DBTTF), 97%	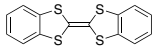	695637-500MG
Bis(ethylenedithio)tetrathiafulvalene (BEDT-TTF), 98%	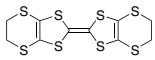	362026-500MG
5,5'-Di(4-biphenylyl)-2,2'-bithiophene, 97%	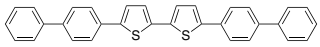	695947-1G
5,5'-Bis(2-hexyl-9*H*-fluoren-7-yl)-2,2'-bithiophene (DHFTTF)	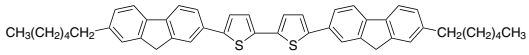	703729-500MG
5,5''''-Dihexyl-2,2':5',2":5",2''':5''',2'''':5'''',2''''-sexithiophene (DH-6T)	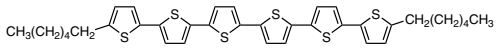	633216-500MG

Dielectric Materials

For a complete list of high-quality polymer materials that can be used as gate-insulators (dielectrics) in OTFTs, please visit us at ***sigma-aldrich.com/polymer***

Name	Structure	Property/Purity	Cat. No.
Polystyrene		average M_w 35,000	331651-25G 331651-500G
		average M_n ~170,000 average M_w ~350,000	441147-1KG
Poly(4-vinylphenol)	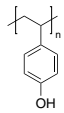	average M_w ~25,000	436224-5G 436224-25G
Poly(methyl methacrylate)	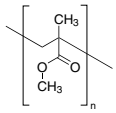	average M_n 46,000 (Typical) average M_w 97,000 (Typical)	370037-25G
		average M_w ~350,000 by GPC	445746-25G 445746-500G 445746-1KG
Poly(4-vinylphenol-*co*-methyl methacrylate)	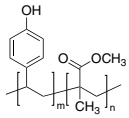	-	474576-50G
Poly[4,5-difluoro-2,2-bis(trifluoromethyl)-1,3-dioxole-*co*-tetrafluoroethylene]	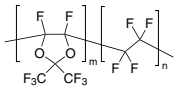	contact angle 104 ° (with water) critical surface energy 15.7 dynes/cm	469610-1G
		contact angle 105 ° (with water) critical surface energy 15.6 dynes/cm	469629-1G
Hexachlorodisiloxane	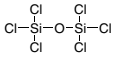	96%	368334-25ML
Bis(trichlorosilyl)methane	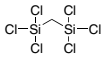	97%	568198-5G
1,2-Bis(trichlorosilyl)ethane	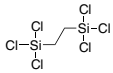	97%	447048-5ML 447048-25ML
1,6-Bis(trichlorosilyl)hexane	$Cl_3SiCH_2(CH_2)_4CH_2SiCl_3$	97%	452246-10G

Substrates for Electronic Devices

Indium Tin Oxide/Indium Oxide Coated Substrates

Product Description	Surface Resistivity (Ω/sq)	L × W × D (mm)	Cat. No.
Indium tin oxide coated aluminosilicate glass slide	5-15	75 × 25 × 1.1	576360-10PAK 576360-25PAK
Indium tin oxide coated glass slide, square	8-12	25 × 25 × 1.1	703192-10PAK
Indium tin oxide coated glass slide, square	30-60	25 × 25 × 1.1	703184-10PAK
Indium tin oxide coated glass slide, square	70-100	25 × 25 × 1.1	703176-10PAK
Indium tin oxide coated glass slide, rectangular	8-12	75 × 25 × 1.1	578274-10PAK 578274-25PAK
Indium tin oxide coated glass slide, rectangular	15-25	75 × 25 × 1.1	636916-10PAK 636916-25PAK
Indium tin oxide coated glass slide, rectangular	30-60	75 × 25 × 1.1	636908-10PAK 636908-25PAK
Indium tin oxide coated glass slide, rectangular	70-100	75 × 25 × 1.1	576352-10PAK 576352-25PAK
Indium tin oxide coated PET	45	1 ft × 1 ft × 5 mm	668559-1EA 668559-5EA
Indium tin oxide coated PET	60	1 ft × 1 ft × 5 mm	639303-1EA 639303-5EA
Indium tin oxide coated PET	100	1 ft × 1 ft × 5 mm	639281-1EA 639281-5EA
Indium oxide coated PET	≤10	150 × 150 × 0.2	700177-5PAK 700177-10PAK
Indium oxide coated PET	60-100	150 × 150 × 0.2	702811-5PAK 702811-10PAK

Polytriarylamine Semiconductors


Iain McCulloch and Martin Heeney
Flexink Limited - www.flexink.co.uk
Southampton, UK
E-mail: sales@flexink.co.uk

Application of Solution Processable Organic Semiconductors in Organic Electronics

Organic electronics is an emerging scientific field of potentially huge technological and commercial relevance[1], and is an increasingly ubiquitous research activity globally. One important area is the development of organic field effect transistors (OFET) which can potentially be employed in applications such as RFID tags and display backplanes.[2,3] In order to be commercially competitive, these devices must be printed by a low-cost, high throughput process. Additive solution based printing techniques such as ink-jet and contact printing are considered to be attractive processing options. In order to satisfy these printing requirements, the semiconductor material should be formulated into an ink, with appropriate rhelology. There are several potentially high performing semiconductors that have been disclosed in the literature recently that can be deposited from solution into thin films.[4-7] In almost all cases, however, aggressive and environmentally unfriendly solvents are required to fully dissolve these crystalline polymers, without which potentially difficult suspensions or gels can form.[8] Additionally, the device fabrication process typically requires a pre-treatment step to reduce the energy of the coating surface, as well as a thermal annealing step after semiconductor deposition to induce optimal crystallinity.[9] Both these additional steps potentially add cost to the process. Another drawback with some thiophene based polymers is that the high electron density over extended conjugation lengths leads to high lying HOMO energy levels with corresponding susceptibility to electrochemical oxidation in ambient conditions. Even in situations where acceptable ambient stability is demonstrated in storage conditions, devices that are driven at high current density conditions or where a bottom-gate transistor architecture is employed, where the semiconductor film is the exposed surface, suffer from instabilities. These instabilities manifest as a deterioration in the large initial carrier mobilities to significantly lower values over short periods.[10] Clearly then, there is a demand for fully air stable polymers that can be easily deposited from environmentally friendly solvents, do not require further treatment to obtain optimal performance and have the flexibility to be employed in any device architecture. Polytriarylamines fit these requirements: they are highly soluble, amorphous semiconducting polymers[11] which require no annealing and can achieve stable charge carrier mobilities of the order of 5×10^{-3} cm^2/Vs in both top and bottom gate transistor architectures.[12] The presence of the amine nitrogen in the polymer backbone acts to prevent efficient delocalization of π electrons between adjacent phenyl units, thus limiting the effective conjugation length and resulting in low lying HOMO energy levels and excellent oxidative stability. The non-planar, rotationally-free and large linkage angle backbone however prevents optimal intermolecular π-electron aromatic stacking, leading to an amorphous microstructure and limiting the charge carrier mobility to lower values than some highly ordered crystalline materials. However, this ease of processing and robust electrical performance offers significant compensation.

Synthesis

Poly(bis(4-phenyl)(2,4,6-trimethylphenyl)amine) (**Aldrich Prod. No. 702471**) was synthesised by palladium catalysed Suzuki coupling, as shown in **Figure 1**. To eliminate the effects of unbalanced stoichiometry, a homo-condensation reaction was employed with the asymmetrically bifunctionalized bromo boronate of the triarylamine repeat unit. Purification of the crude polymer is essential, affording the polymer as yellow solid, soluble in common organic solvents such as tolulene (**Aldrich Prod. No. 568821**), chloroform (**Aldrich Prod. No. 372978**) and xylene (**Aldrich Prod. No. 296333**). Number average molecular weights of over 45 Kda can be obtained by this procedure, with polydispersities of between 2 and 3.

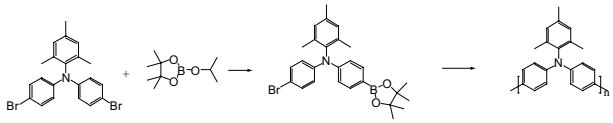

Figure 1. Synthesis of Poly(bis(4-phenyl)(2,4,6-trimethylphenyl)amine) by palladium catalyzed Suzuki coupling.

Transistor Devices

Field effect transistor devices were fabricated on a glass substrate (Corning EAGLE 2000) using a bottom-contact, top-gate architecture, often referred to as a staggered geometry, as shown in **Figure 2**. The glass was cleaned by sonication in a detergent solution. Source and drain electrodes were evaporated Au treated with a pentafluorobenzenethiol (PFBT) (**Aldrich Prod. No. P3033**) self-assembled monolayer. Typical channel dimensions were 30 µm length and 1000 µm width. Polymers were spin coated from a 10 mg/ml solution in chlorobenzene at 2000 rpm and dried at 100°C for 2 min. The gate dielectric was a fluoropolymer CYTOP and again deposited by spin coating from a 9 wt% solution in FC43 solvent, and dried at 100°C. Top-gate electrodes were evaporated aluminum. Device fabrication was carried out under nitrogen with storage and electrical testing in air for the stability tests.

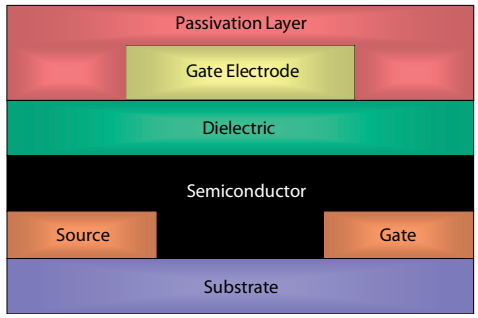

Figure 2. Top gate, staggered contact transistor architecture

Transistors were characterised using a Keithley 4200 semiconductor parameter analyzer. Saturation mobilities were calculated using a standard thin film transistor model according to the equation below:

$$\mu_{sat} = \frac{\partial^2 I_{Dsat}}{\partial V_G^2} \frac{L}{WC_i}$$

where C_i is the geometric capacitance of the gate dielectric (2.1 nFcm^{-2}). Carrier mobilities of 5x10^{-3} cm^2/Vs were extracted from the current-voltage characteristics shown in **Figure 3**. The transfer characteristics of a typical device is shown in **Figure 3(a)**, with ON/OFF ratios of about 10^4 and a threshold voltage close to 0 V. As illustrated in the linear shape of output characteristics at low source drain voltage (**Figure 3(b)**) the PFBT electrode treatment successfully lowers the Au work function, thus ensuring that there are no contact injection problems.

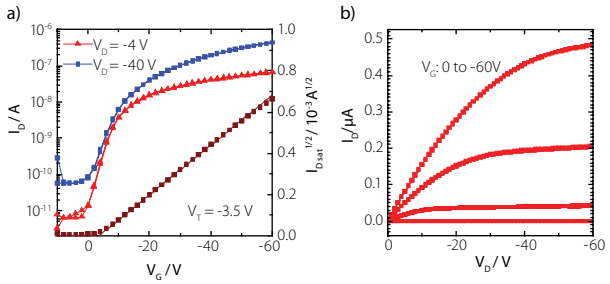

Figure 3. Transfer (**a**) and output (**b**) characteristics of a PTAA top-gate bottom-contact device with Cytop dielectric and Au source and drain electrodes treated with pentafluorobenzenethiol. Channel length (L) was 30 microns and width (W) was 1000 microns corresponding to a charge carrier mobility of 5 x 10^{-3} cm^2/Vs.

Conclusion

Polyarylamines are a versatile class of air stable, solution processable organic semiconductors. Their performance has been shown to be inert to ambient air and humidity, which for long term operation provides sustained and consistent currents, outperforming most of the less stable semiconductors. Their amorphous nature contributes to high solubility in a range of formulation solvents, with many choices outside the typical chlorinated aromatic solvents necessary for dissolution of highly crystalline thiophene containing polymers. Neither surface alignment layers, or high temperature annealing are required to obtain optimal performance, illustrating the flexible nature of these polymers.

References:

(1) Loo, Y.-L.; McCulloch, I. *MRS Bull.* **2008**, *33*, 653-662.
(2) Cantatore, E.; Geuns, T. C. T.; Gelinck, G. H.; van Veenendaal, E.; Gruijthuijsen, A. F. A.; Schrijnemakers, L.; Drews, S.; de Leeuw, D. M. *Solid-State Circuits, IEEE Journal of* **2007**, *42*, 84-92.
(3) Chabinyc, M. L.; Salleo, A. *Chem. Mater.* **2004**, *16*, 4509-4521.
(4) Yan, H.; Chen, Z.; Zheng, Y.; Newman, C.; Quinn, J. R.; Dotz, F.; Kastler, M.; Facchetti, A. *Nature* **2009**, *457*, 679-686.
(5) McCulloch, I.; Heeney, M.; Bailey, C.; Genevicius, K.; MacDonald, I.; Shkunov, M.; Sparrowe, D.; Tierney, S.; Wagner, R.; Zhang, W.; Chabinyc, M. L.; Kline, R. J.; McGehee, M. D.; Toney, M. F. *Nat. Mater.* **2006**, *5*, 328-333.
(6) Li, J.; Qin, F.; Li, C. M.; Bao, Q.; Chan-Park, M. B.; Zhang, W.; Qin, J.; Ong, B. S. *Chem. Mater.* **2008**, *20*, 2057-2059.
(7) Tsao, H. N.; Cho, D.; Andreasen, J. W.; Rouhanipour, A.; Breiby, D. W.; Pisula, W.; Müllen, K. *Adv. Mater.* **2009**, *21*, NA.
(8) Koppe, M.; Brabec, C. J.; Heiml, S.; Schausberger, A.; Duffy, W.; Heeney, M.; McCulloch, I. *Macromolecules* **2009**, *42*, 4661-4666.
(9) DeLongchamp, D. M.; Kline, R. J.; Jung, Y.; Lin, E. K.; Fischer, D. A.; Gundlach, D. J.; Cotts, S. K.; Moad, A. J.; Richter, L. J.; Toney, M. F.; Heeney, M.; McCulloch, I. *Macromolecules* **2008**, *41*, 5709-5715.
(10) Mathijssen, S. G. J.; Coelle, M.; Gomes, H.; Smits, E. C. P.; de Boer, B.; McCulloch, I.; Bobbert, P. A.; de Leeuw, D. M. *Adv. Mater.* **2007**, *19*, 2785-2789.
(11) Veres, J.; Ogier, S. D.; Leeming, S. W.; Cupertino, D. C.; Khaffaf, S. M. *Adv. Funct. Mater.* **2003**, *13*, 199-204.
(12) Zhang, W.; Smith, J.; Hamilton, R.; Heeney, M.; Kirkpatrick, J.; Song, K.; Watkins, S. E.; Anthopoulos, T.; McCulloch, I. *J. Am. Chem. Soc.* **2009**, 131, 10814-10815.

Polymeric Semiconductors

For a complete range of organic semiconductor materials, please visit ***sigma-aldrich.com/semiconductors***

p-Type Semiconductors

Name	Structure	Mobility	Average Molecular Weight	Cat. No.
Poly[bis(4-phenyl)(2,4,6-trimethylphenyl) amine]	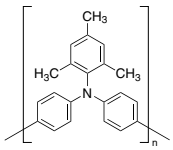	10^{-3} - 10^{-2} cm^2/V·s	average M_n 7,000-10,000 (GPC)	702471-100MG 702471-1G
Poly[(9,9-di-*n*-octylfluorenyl-2,7-diyl)-*alt*-(benzo[2,1,3]thiadiazol-4,8-diyl)]	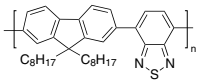	4×10^{-3} cm^2/V·s	average M_n 5,000-8,000	698687-250MG
Poly[(9,9-dioctylfluorenyl-2,7-diyl)-*co*-bithiophene]	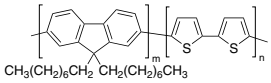	5×10^{-3} cm^2/V·s	average M_n >20,000	685070-250MG
Poly(3-hexylthiophene-2,5-diyl)	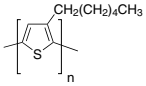	10^{-4} - 10^{-1} cm^2/V·s	average M_n 25,000-35,000	698989-250MG 698989-1G
		10^{-4} - 10^{-1} cm^2/V·s	average M_n 45,000-65,000	698997-250MG 698997-1G
Poly(3-octylthiophene-2,5-diyl)	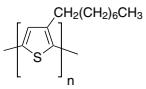	10^{-4} - 10^{-1} cm^2/V·s	average M_n ~25,000	682799-250MG
Poly(3-dodecylthiophene-2,5-diyl)	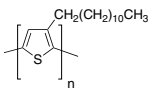	10^{-4} - 10^{-1} cm^2/V·s	average M_w ~27,000	682780-250MG

n-Type Semiconductors

Name	Structure	Average Molecular Weight	Cat. No.
Poly(benzimidazobenzophenanthroline)	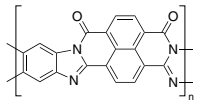	-	667846-250MG 667846-1G
Poly[(1,4-divinylenephenylene) (2,4,6-triisopropylphenylborane)]	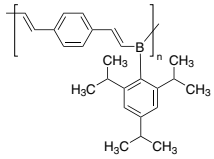	average M_n ~1379	688010-250MG
Poly[(2,5-didecyloxy-1,4-phenylene) (2,4,6-triisopropylphenylborane)], diphenyl terminated	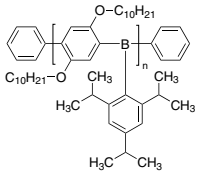	average M_n ~1446	688002-250MG

New Synthetic Intermediates

A complete range of synthetic tools can be found at ***sigma-aldrich.com/synthetic***

Name	Structure	Purity	Cat. No.
Thieno[2,3-*b*]thiophene		95%	702641-1G 702641-5G
Thieno[3,2-*b*]thiophene		95%	702668-1G 702668-5G
2,5-Dibromothieno[3,2-*b*]thiophene	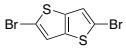	≥98%	710164-1G
Dithieno[3,2-*b*:2′,3′-*d*]thiophene		97%	710172-500MG
2-Bromo-3-hexylthiophene	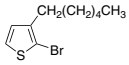	97%	691925-1G 691925-5G
2-Bromo-3-octylthiophene	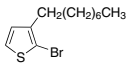	97%	714550
2-Bromo-3-dodecylthiophene	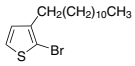	95%	688312-1G
5-Bromo-2-hexylthiophene	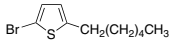	97%	694258-1G
2,5-Dibromo-3-hexylthiophene	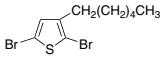	97%	456373-1G 456373-5G
5,5″-Dibromo-2,2′:5′,2″-terthiophene	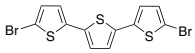	97%	699098-500MG
2-Bromo-7-hexyl-9*H*-fluorene	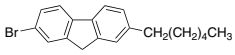	97%	701254-1G
trans-4,4′-Dibromostilbene	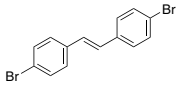	98%	705721-1G
4,4′-biphenyldiboronic acid bis(neopentyl) ester	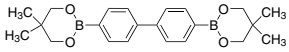	97%	704318-1G

Name	Structure	Purity	Cat. No.
4,4′-Biphenyldiboronic acid bis(pinacol) ester	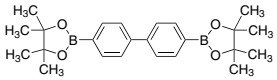	97%	704199-1G
2,1,3-Benzothiadiazole-4,7-bis(boronic acid pinacol ester)	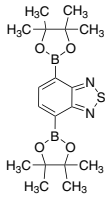	95%	702803-1G
4,7-Dibromobenzo[*c*]-1,2,5-thiadiazole		95%	693847-1G 693847-5G
5-Fluoro-2,3-thiophenedicarboxaldehyde		97%	708283-500MG
4,4′-Dibromotriphenylamine	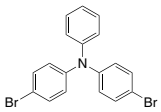	96%	679917-1G 679917-5G
2,8-Dibromo-6,12-dihydro-6,6,12,12-tetraoctyl-indeno[1,2-*b*]fluorene	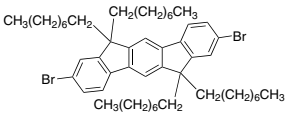	>95%	708267-500MG

Organic Semiconductor Laser Materials


Chihaya Adachi*, Hajime Nakanotani
Center for Future Chemistry, Kyushu University, Fukuoka City, Japan
*E-mail: adachi@cstf.kyushu-u.ac.jp

Abstract

Over recent years, a wide variety of challenges aiming for electrical pumping of organic laser diodes have been addressed. However, organic laser diodes have difficulty gaining widespread application due to their high lasing thresholds under electrical pumping. A variety of organic semiconductors have been developed to reduce the lasing threshold, which include not only small molecular materials but also conjugated polymers. In this article, we demonstrate that bis-styrylbenzene derivatives show promising characteristics for very low lasing thresholds and discuss the design considerations for organic lasing molecules.

Introduction

The dissolution of luminescent organic dye molecules in an organic solvent followed by their excitation with high-energy light (greater than their lasing threshold) produces a laser beam. Due to their broad tunabilities, dye lasers have made remarkable advancements.[1-5] In recent years, organic solid-state lasers involving the dispersion of an organic dye within a solid/crystal matrix have also been actively studied. In 1989, we proposed an idea to create an organic semiconductor laser diode using triplet excitons of rare earth complexes such as a europium (Eu) complex.[6] This system would produce an electrically excited laser with a low threshold by forming a population inversion using the long excitation lifetime of Eu. There have been many studies reporting amplified spontaneous emission (ASE) oscillation from an organic solid thin film and laser oscillation from an organic thin film with an oscillator structure. The thin films in these studies were made by doping a polymer or small-molecule medium with an appropriate laser dye.[7-11] These studies provide evidence that organic dyes have suitably high stimulated emission coefficients and that the formation of a solid thin film waveguide can provide the necessary architecture for a solid-state device with a low lasing threshold. More recently, laser oscillations from organic semiconductor dyes, which take electrical excitation into consideration, have also been actively studied.[12,13] This interest was generated because organic light-emitting diodes (OLEDs) have achieved an internal luminescence efficiency of nearly 100% through the use of a triplet excited state at the luminescence center. This excited state leads to the realization of an organic semiconductor laser that is an extension of OLEDs a practical study subject of organic electronics.[14] In addition, light-emitting transistors have also become capable of producing highly efficient electroluminescence (EL), prompting new electrical excitation developments of organic semiconductors.[14-21] In this article, we will discuss materials issues for the production of an organic semiconductor laser. This process requires the development of a new laser material with a focus on a low lasing threshold. Derivatives of bis-styrylbenzene (BSB) have demonstrated extremely good ASE oscillation characteristics in organic solid thin films.[15,16] As a result, we will introduce new organic semiconductor materials with similar ASE characteristics in organic solid thin films by using BSB analogs as active materials.

The Mechanism and Goal of Organic LEDs

The external quantum efficiency (η_{ext}) of OLEDs is based on four factors: (i) the ratio of electron and hole injection, transport, and recombination (v), (ii) exciton formation efficiency (η_r), (iii) internal electroluminescence quantum yield (φ_p), and (iv) light out-coupling efficiency (η_p) (**Figure 1**).

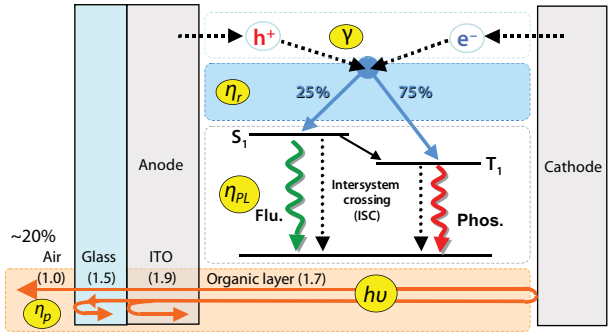

Figure 1. OLED luminescence processes (carrier injection, transport, recombination, exciton formation/decay, and light extraction) and their efficiencies. Figures in parentheses represent refractive indices.

Obtaining the highest possible luminescence efficiency requires bringing each of the four factors as close to 100% as possible. Here, v is a physical quantity containing the ratio of electron and hole injection and transport, as well as the probability of electron and hole recombination. φ_p can have a value near to 100% by using a material with a high internal luminescence quantum yield. Although η_r is generally low (25% when fluorescent materials are used), the use of phosphorescent materials can theoretically provide an η_r of 75 to 100%. If a device is formed on a common glass substrate, η_p is low at about 20%. Therefore, if fluorescent materials are used as luminescent molecules, η_{ext} is approx 5% at most, but with the use of a triplet exciton as a luminescence transition process can provide a luminescence efficiency theoretically 3 or more times higher. In instances where the intersystem crossing (ISC) probability is about 100%, a luminescence efficiency approximately 4 times higher can be acheived. **Figure 2** shows typical luminescent materials used in OLEDs.

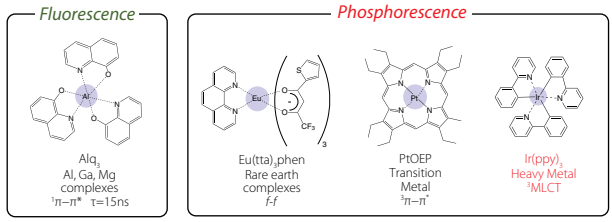

Figure 2. Fluorescent and phosphorescent materials used in OLEDs

For Alq_3 (**Aldrich Prod. No. 444561**) and DPVBi, luminescence is found during the transition from the excited singlet state to the ground state. In contrast, for Eu (**Aldrich Prod. No. 538957**), platinum (Pt) (**Aldrich Prod. No. 673625**), and iridium (Ir) (**Aldrich Prod. No. 688096**) complexes, all singlet excitons undergo intersystem crossing into triplet excitons due to the internal heavy atom effect. In the triplet state, a radiative transition occurs with high luminescence efficiency. Use of an Ir compound at the luminescence center reportedly provides a high external EL quantum yield (η_{ext}) of greater than 20%, showing that the internal quantum yield (η_{int}) reaches almost 100%.[22] As described above, the electrons and holes injected into the organic layer result in almost immediate exciton formation.

Laser Active Materials (Fluorescent and Phosphorescent Materials)—Population Inversion Formation at a Low Threshold

To investigate various organic laser materials, we synthesized a variety of styrylamine-, coumarin-, and cyanine-based materials. Here, we will discuss the light amplification characteristics (ASE characteristics) of styrylbenzene derivatives, which we believe to be the most promising laser materials.[15,16] **Figure 3** presents a selection of the molecules that were studied.

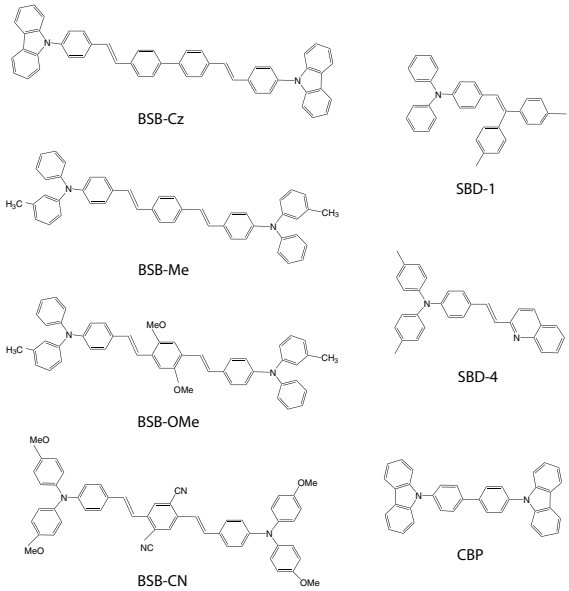

Figure 3. Styrylbenzene-based organic laser materials

Table 1 shows the ASE characteristics of thin films that are 6 wt% doped with styrylbenzene-based luminescent materials under optical excitation with 4,4′-bis[9-dicarbazolyl]-2,2′-biphenyl (CBP) (**Aldrich Prod. No. 660124**) as the host. Typical BSB which have a dimer skeleton often exhibit especially low threshold ($E_{th} \cong 1.0$ μJ/cm^2). Molecules with a heterocycle have an ASE threshold of 20 to 100 μJ/cm^2, and molecules with an azomethine skeleton do not cause emission spectrum narrowing even with an excitation energy >100 μJ/cm^2. To identify the controlling factors of ASE thresholds, data values for absolute photoluminescence quantum efficiency (φ_f), fluorescence lifetime (τ_f), radiative decay constant (k_r), and triplet-triplet absorption are shown in **Table 1**.

Table 1. Basic optical physical characteristics of styryl-based laser materials

	λ_{ASE} (nm)	Φ_{PL} (%)	τ (ns)	k_r ($\times 10^8 s^{-1}$)	E_{th} (μJ/cm^2)	σ_{em} ($\times 10^{-16} s^{-1}$)
SBD-1	474	62±3	1.8	3.4	1.2±0.20	0.97
SBD-4	504	92±2	2.2	4.4	9.5±1.0	1.54
BSB-Cz	462	99±1	1.0	10	0.32±0.05	2.70
BSB-Me	505	92±3	1.0	9.1	0.78±0.10	2.66
BSB-OMe	530	90±1	1.2	7.2	0.90±0.10	2.33
BSB-CN	586	55±2	1.5	3.7	2.35±0.10	1.84

The ASE thresholds are not directly correlated with φ_f or τ_f but are greatly correlated with k_r. The magnitude of k_r can determine how large the threshold is. 4,4′-bis[(N-carbazole)styryl]biphenyl (BSB-Cz) has extremely good ASE characteristics. The threshold of BSB-Cz is the lowest of the styryl-based fluorescent materials studied so far.[15] The luminescence intensity and lifetime do not depend on temperature, so the nonradiative decay is completely inhibited, even at room temperature. The ASE oscillation wavelength of BSB-Cz corresponds to the 0-1 transition in the PL spectrum. The radiative decay constant (k_r), stimulated emission cross-section (σ_{em}), and absorption cross-section (σ_{ABS}) are calculated as below. k_r (= η_{PL}/τ_f) is calculated with the fluorescence lifetime (τ_f) and luminescence quantum efficiency (η_{PL}) of each codeposited thin film. σ_{em} is given by equations (**1**) and (**2**) below with the absolute luminescence quantum yield and fluorescence lifetime of each codeposited thin film:[24,25]

$$\sigma_{em}(\lambda) = \frac{\lambda^4 E_f(\lambda)}{8\pi n^2(\lambda) c \tau_f} \quad (1)$$

$$n_f = \int E_f(\lambda) d\lambda \quad (2)$$

where, $E_f(\lambda)$ is quantum yield distribution, n (λ) is the refractive index of each wavelength, and τ_f is fluorescence lifetime. When the refractive index n = 1.8, the absorption cross-section σ_{ABS}[26] is given by equation (**3**) below:

$$\sigma_{ABS,sol}(\lambda) = \frac{1000\varepsilon(\lambda) \ln 10}{N_A} \quad (3)$$

where, ε(λ) is the molar absorption coefficient, and N_A is Avogadro's number. k_r and σ_{em} are strongly correlated with the ASE oscillation threshold E_{th} in each codeposited thin film. The ASE oscillation thresholds in thin films with the dimmers BSB-Cz, BSB-Me, and BSB-OMe as active materials are 1 μJ/cm^2 or less. The 6 wt%-BSB-Cz:CBP thin film's σ_{em} is the highest. Although the SBD-4:CBP codeposited thin film is higher in k_r and σ_{em} than the SBD-1:CBP codeposited thin film, SBD-4:CBP has a high oscillation threshold E_{th} and the saturation of luminescence intensity is noted at high excitation intensity.
This suggests that there is a factor inhibiting luminescence in the 6 wt%-SBD-4:CBP codeposited thin film. Here, the effective stimulated emission cross-section is the difference between the stimulated emission cross-section and loss-related cross-sections (absorption cross-section and excited-state absorption cross-sections) and is given by equation (4) below:

$$\sigma_{emeff} = \sigma_{em} - (\sigma_{ABS} + \sigma_{SS} + \sigma_{TT}) \quad (4)$$

where, σ_{emeff} is the effective stimulated emission cross-section, σ_{em} is the stimulated emission cross-section, σ_{SS} is the singlet excited-state absorption cross-section, and σ_{TT} is the triplet excited-state absorption cross-section. The absorption cross-section at the ASE oscillation wavelength of the SBD-4:CBP codeposited thin film is negligible, meaning that the excited-state absorption has a great impact on σ_{emeff}. Singlet and triplet excited-state absorption is found in any of the codeposited thin films, and the ASE oscillation wavelength of SBD-1 has triplet excited-state absorption, but not singlet excited-state absorption. In contrast, SBD-4 has singlet and triplet excited-state absorption in the luminescence wavelength range. This result shows that the occurrence of singlet excitation absorption under strong excitation inhibits the formation of population inversion, resulting

in no stimulated emission. **Figure 4** shows the stimulated emission and absorption cross-sections spectra and excited-state absorption spectrum of the 6 wt%-BSB-Cz:CBP codeposited thin film that has the lowest ASE oscillation threshold. For BSB-Cz, neither the single nor triplet excited-state absorption exists at the ASE oscillation wavelength, providing materials designed to perform at low thresholds.

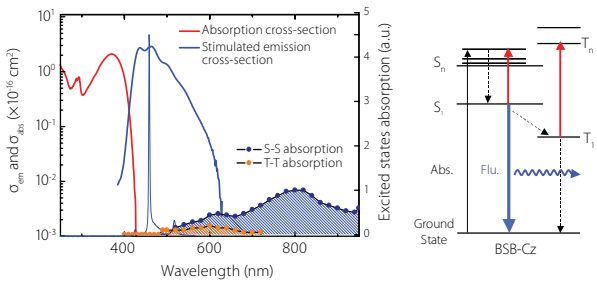

Figure 4. ASE spectrum and S-S and T-T absorption spectra of BSB-Cz

Development to An Electrically Excitable Device Structure

OLED and FET structures also show promise in realizing an organic semiconductor laser. The OLED structure is basically a double heterostructure to effectively trap electrons and holes as well as trapping generated excitons within the luminescent layer. Advantages of this structure include the ability to use the OLED design guidelines developed so far and the flexibility to select a wide range of organic materials. However, a drawback of this structure is the failure to guide light effectively if a metal electrode is used as the cathode. Therefore, a transparent electrode such as ITO needs to be used at both the anode and cathode. For example, when a transparent device structure with ITO (30 nm)/a-NPD (20 nm)/CBP:BSB [6 wt%] (70 nm)/BCP (20 nm)/Alq_3 (20 nm)/MgAg (X nm)/ITO (30 nm)[15] is used, a clear ASE oscillation is noted under optical excitation as long as the MgAg layer is between 1 and 3 nm thick (**Figure 5**).

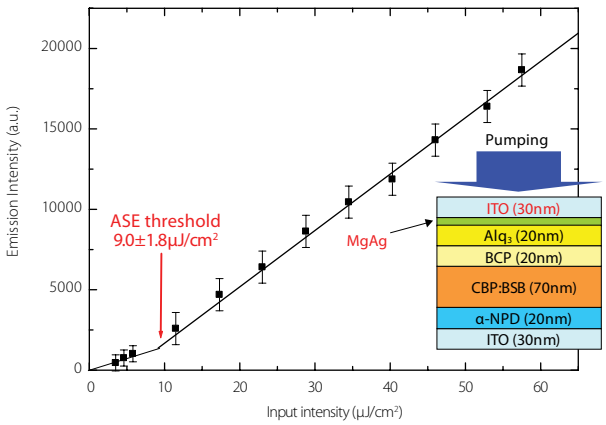

Figure 5. ASE characteristics under the excitation of light from an electrically excitable laser structure

Recently, even transistor structures have allowed luminescent devices to be constructed. Light emission has actually been observed near the drain electrode by using p-type organic semiconductors such as oligothiophene[27], tetracene[28] (**Aldrich Prod. No. 698415**), fluorene-based polymers (**Aldrich Prod. No. 571032**), PPV-based polymers[29] (**Aldrich Prod. No. 541443**), and thiophene-based oligomers[30] (**Figure 6**).

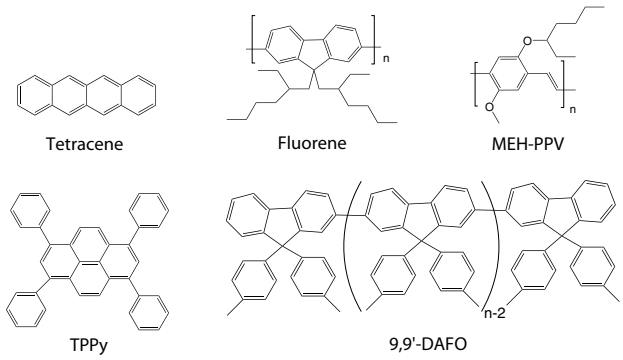

Figure 6. Organic semiconductor materials for light-emitting transistors

Also, use of a tetraphenylpyrene derivative (TPPy) has dramatically improved luminescence efficiency with an external EL efficiency of 1%.[31] These devices are unipolar light-emitting transistors, and their operation mechanism is shown in **Figure 7-1**. Application of a gate voltage allows holes to accumulate between the electrodes and the organic layer, and an increase in the voltage between the source and drain electrodes allows a region with no hole accumulation (known as a pinch-off region) to be formed near the drain electrode. A strong electric field is created at the interface between the drain electrode and the pinch-off region, accelerating the electron injection.

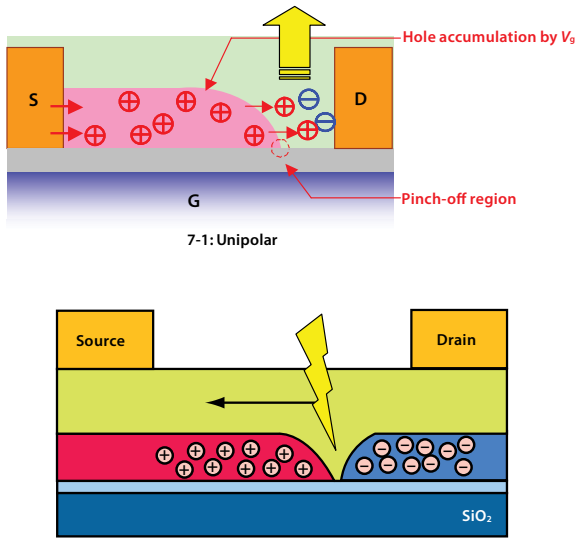

Figure 7. Schematics and operation mechanisms of light-emitting transistors

In addition, the development of ambipolar organic semiconductors has lead to higher EL efficiency, and some ambipolar devices (**Figure 7-2**) have been fabricated with polymer organic semiconductors.[32,33] Even in a small-molecule system, a clear electroluminescence has been observed (**Figure 8**) when a single-crystal from a BSB derivative with a simple molecular frame[34] is used. Application of an appropriate gate voltage provides electroluminescence between the source and drain electrodes.

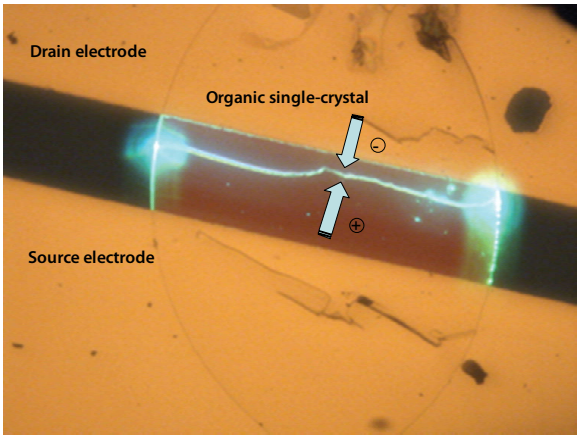

Figure 8. Ambipolar FET producing bright electroluminescence

This ambipolar type architecture also has many advantages over OLEDs and shows promise as a future device structure for organic semiconductor lasers. Transistors using organic substances have been studied since the early 1980s when a pioneering organic transistor was first reported.[35] As findings about materials and devices have accumulated rapidly, the use of fused polycyclic aromatic compounds such as tetracene and rubrene (**Aldrich Prod. No. 554073**) have recently achieved an electron field-effect mobility of about 10 cm^2/Vs. Electroluminescence from devices using a transistor structure has a high electronic and optical freedom, and are therefore suitable for organic semiconductor lasers, holding promise for future developments.

References:

(1) Sorokin, P. P.; Lankard, J. R. *IBM J. Res. Develop.* **1966**, *10*, 162-163.
(2) Schäfer, F. P.; Schmidt, W.; Volze, J. *Appl. Phys. Lett.* **1966**, *9*, 306 -309.
(3) Soffer B. H.; McFarland, B. B. *Appl. Phys. Lett.* **1967**, *10*, 266-267.
(4) Sorokin, P. P.; Lankard, J. R.; Moruzzi, V. L.; Hammond, E. C. *J. Chem. Phys.* **1968**, *48*, 4726-4741.
(5) Sorokin, P. P.; Lankard, J. R.; Moruzzi, V. L.; Lurio, A. *Appl. Phys. Lett.* **1969**, *15*, 179-181.
(6) Chihaya Adachi, Student Advanced technical paper, 1989, Nippon Kogyo Shinbun
(7) Tessler, N.; Denton, G. J.; Friend, R. H. *Nature* **1996**, *382*, 695-697.
(8) Frolov, S. V.; Ozaki, M.; Gellermann, W.; Vardeny, Z. V.; Yoshino, K. *Jpn. J. Appl. Phys.* **1996**, *35*, L1371- L1373.
(9) Hide, F.; diaz-García, M. A.; Schwartz, B. J.; Andersson, M. R.; Pei, Q.; Heeger, A. J. *Science* **1996**, *273*, 1833-1836.
(10) Kozlov, V. G.; Bulovic, V.; Burrows, P. E.; Forrest, S. R.; *Nature* **1997**, *389*, 362-364.
(11) Berggren, M.; Dodabalapur, A.; Slusher, R. E.; Bao, Z.; *Nature* **1997**, *389*, 466-469.
(12) Tessler, N. *Adv. Mater.* **1999**, *5*, 363-370.
(13) Yamamoto, H.; Oyamada, T.; Sasabe, H.; Adachi, C. *Appl. Phys. Lett. 84*, 1401-1403.
(14) Adachi, C.; Baldo, M. A.; Forrest, S. R. *J. Appl. Phys.* **2001**, *90*, 5048-8055.
(15) Aimono, T.; Kawamura, Y.; Goushi, K.; Yamamoto, H.; Sasabe, H.; Adachi, C. *Appl. Phys. Lett.* **2005**, *86*, 071110-071112.
(16) Nakanotani, H.; Sasabe, H.; Adachi, C. *Proc. SPIE Int. Soc. Opt. Eng.* **2005**, *5937*, 59370W-1-7.
(17) Yamamoto, H.; Kasajima, H.; Yokoyama, W.; Sasabe, H.; Adachi, C. *Appl. Phys. Lett.* **2005**, *86*, 083502-083504.
(18) Nakanotani, H.; Oyamada, T.; Kawamura, Y.; Sasabe, H.; Adachi, C. *Jpn. J. Appl. Phys.* **2005**, *44*, 3659-3662.
(19) Baldo, M. A.; Adachi, C.; Forrest, S. R. *Phys. Rev. B* **2000**, *62*, 109671-10977.
(20) Baldo, M. A.; Holmes, R. J.; Forrest, S. R. *Phys. Rev. B* **2002**, *66*, 035321.
(21) Nakanotani, N.; Sasabe, H.; Adachi, C. *Appl. Phys. Lett.* **2005**, *86*, 213506-1-3.
(22) Adachi, C.; Baldo M. A.; Forrest, S. R. *J. Appl. Phys.* **2001**, *90*, 5048-5051.
(23) Yokoyama, W.; Sasabe, H.; Adachi, C. *Jpn. J. Appl. Phys.* **2003**, *42*, L1353-1355.
(24) Deshpande, A.; Deshpande, V.; Beidoun, A.; Penzkofer, A.; Wagenblast, G. *Chem. Phys.* **1990**, *142*, 123-131.
(25) Holzer, W.; Penzkofer, A.; Schmitt, T.; Hartmann, A.; Bader, C.; Tillmann, H.; Raabe, D.; Stockmann, R.; Hörhold, H.-H. *Opt. Quantum Electron* **2001**, *33*, 121-150.
(26) Liu, X.; Py, C.; Tao, Y.; Li, Y.; Ding, J.; Day, M. *Appl. Phys. Lett.* **2004**, *84*, 2727-2729.
(27) Shaklee K. L.; Leheny, R. F. *Appl. Phys. Lett.* **1971**, *18*, 475-305.
(28) Schön, J. H.; Kloc, Ch.; Haddon R. C.; Batlogg, B. *Science* **2000**, *288*, 656-658.
(29) Hepp, A.; Heil, H.; Weise, W.; Ahles, M.; Schmechel, R.; von Seggern, H. *Phys. Rev. Lett.* **2003**, *91*, 157406-1-4.
(30) Sakanoue, T.; Fujiwara, E.; Yamada R.; Tada, H. *Appl. Phys. Lett.* **2004**, *84*, 3037-3039.
(31) Oyamada, T.; Okuyama, S.; Shimoji, N.; Matsushige, K.; Sasabe, H.; Adachi, C. *Appl. Phys. Lett.* **2005**, *86*, 093505.
(32) Oyamada, T.; Uchiuzo, H.; Akiyama, S.; Oku, Y.; Shimoji, N.; Matsushige, K.; Sasabe, H.; Adachi, C. *J. Appl. Phys.* **2005**, *98*, 074506-1-7.
(33) Zaumseil, J.; Friend, R. H.; Sirringhaus, H. *Nature Materials* **2006**, *5*, 69-74.
(34) Dinelli, F.; Capelli, R.; Loi, M. A.; Murgia, M.; Muccini, M.; Facchetti A.; Marks, T. J. *Adv. Mat.* **2006**, *18*, 1416-1420.
(35) Nakanotani, H.; Saito, M.; Nakamura H.; Adachi, C. *Appl. Phys. Lett.* **2009**, *95*, 033308.
(36) Kudo, K.; Yamashina, M.; Moriizumi, T. *Jpn. J. Appl. Phys.* **1984**, *23*, 130.

Sublimed Grade Materials for Organic Electronics

Name	Structure	Purity	Spectroscopic Properties	Cat. No.
Anthracene	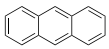	sublimed grade ≥99%	-	694959-5G 694959-25G
Benz[*b*]anthracene	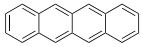	sublimed grade 99.99% trace metals basis	λ_{max} = 277 nm λ_{em} = 481, 514 nm in dichloromethane-d_2	698415-1G
Perylene	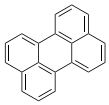	sublimed grade ≥99.5%	λ_{max} = 436 nm λ_{em} = 447 nm in tetrahydrofuran	394475-1G 394475-5G
4,4′-Bis(*N*-carbazolyl)-1,1′-biphenyl	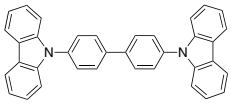	sublimed grade ≥99.99% trace metals basis	λ_{max} = 532 nm	699195-1G
N,N′-Di-[(1-naphthyl)-*N,N*′-diphenyl]-1,1′-biphenyl)-4,4′-diamine	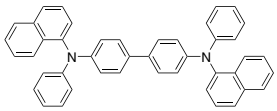	sublimed grade 99%	-	556696-500MG

Name	Structure	Purity	Spectroscopic Properties	Cat. No.
Rubrene	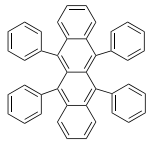	sublimed grade	λ_{max} = 299 nm λ_{em} = 550 nm in tetrahydrofuran	551112-100MG 551112-500MG
Bathocuproine	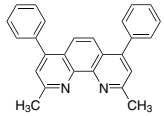	sublimed grade 99.99% trace metals basis	λ_{max} = 277 nm λ_{em} = 386 nm in tetrahydrofuran	699152-500MG
Tris[2-phenylpyridinato-C^2,*N*]iridium(III)	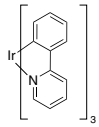	sublimed grade	λ_{max} = 282 nm λ_{em} = 507 nm in chloroform	694924-250MG
Tris[1-phenylisoquinoline-C^2,*N*]iridium(III)	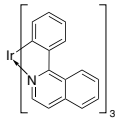	sublimed grade	λ_{max} = 324 nm λ_{em} = 615 nm in tetrahydrofuran	688118-250MG
Tris(dibenzoylmethane) mono(1,10-phenanthroline)europium(III)	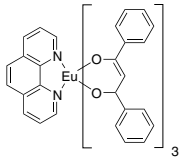	sublimed grade	λ_{max} = 228 nm λ_{em} = 615 nm in tetrahydrofuran	538965-250MG
Tris-(8-hydroxyquinoline)aluminum	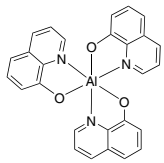	sublimed grade 99.995% trace metals basis	λ_{max} = 259 nm λ_{em} = 519 nm	697737-1G
Copper(II) phthalocyanine	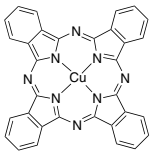	sublimed grade	λ_{max} = 678 nm λ_{em} = 404 nm	546674-1G
		triple-sublimed grade >99.99% trace metals basis	λ_{max} = 678 nm λ_{em} = 404 nm	702854-500MG

Conducting Materials

A complete range of conducting polymers and monomers can be found at ***sigma-aldrich.com/conductors***

Name	Structure	Form (%)	Conductivity (S/cm)	Cat. No.
Poly(3,4-ethylenedioxythiophene)-poly(styrenesulfonate) (PEDOT/PSS)	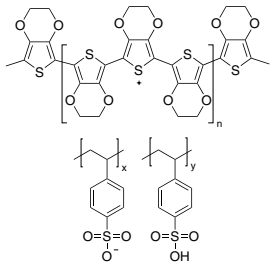	1.3-1.7% in H_2O	150 (18 µm film thickness)	655201-5G 655201-25G
		1.3 wt % dispersion in H_2O	1	483095-250G
		2.8 wt % dispersion in H_2O	~ 1E-5	560596-25G 560596-100G
Poly(thiophene-3-[2-(2-methoxyethoxy) ethoxy]-2,5-diyl), sulfonated solution	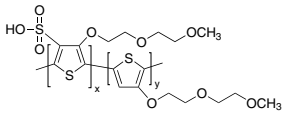	≥99.99, 2% in ethylene glycol monobutyl ether/water, 3:2	-	699780-25ML
		≥99.99, 2% in 1,2-propanediol/ isopropanol	-	699799-25ML

Various Materials for OLED Research

A complete list of OLED and PLED research materials can be found at ***sigma-aldrich.com/oled***

Name	Product Description	Structure	Spectroscopic Properties	Cat. No.
1,3,6,8-Tetrabromopyrene	Synthetic building block for the creation of blue to green OLED emitters	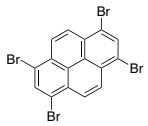	-	717274-5G
1,3-Bis(*N*-carbazolyl) benzene (mCP)	Material for use as a phosphorescent host material	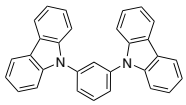	λ_{max} = 292, 338 nm λ_{em} = 345, 360 nm in tetrahydrofuran	701874-5G
2,5-Bis(1-naphthyl)-1,3,4-oxadiazole (BND)	Organic electronic material useful as an electron transporter in organic light emitting diodes (OLEDs).	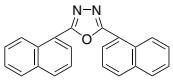	-	698202-5G
Coumarin 6	Material used as Green Dopant	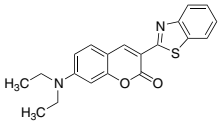	λ_{max} = 443 nm λ_{em} = 494 nm in tetrahydrofuran	546283-100MG
5,12-Dihydro-5,12-dimethylquino[2,3-*b*]acridine-7,14-dione (DMQA)	When used as the emissive dopant in an Alq host layer, DMQA provides improved operational stability.	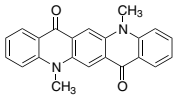	λ_{max} = 295 nm in methylene chloride	557587-100MG 557587-500MG
3,5-Diphenyl-4-(1-naphthyl)-1*H*-1,2,4-triazole (TAZ)	Electron Transport Layer (ETL) material	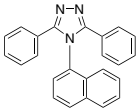	λ_{max} = 264 nm λ_{em} = 367 nm in dichloromethane-d_2	703761-1G
Bis(8-hydroxy-2-methylquinoline)-(4-phenylphenoxy) aluminum (BAlq)	Electron Transport Layer (ETL) material	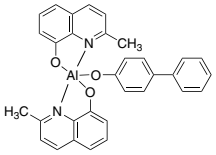	λ_{max} = 259 nm λ_{em} = 334, 477 nm in tetrahydrofuran	704571
Tris[2-(benzo[*b*]thiophen-2-yl)pyridinato-C^3,*N*] iridium(III) (*fac*-Ir(btpy)$_3$)	OLED triplet emitter (red).	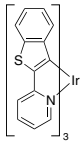	λ_{max} = 324 nm λ_{em} = 595 nm	680877-250MG
Tris[2-(4,6-difluorophenyl) pyridinato-C^2,*N*] iridium(III) (Ir(Fppy)$_3$)	OLED triplet emitter (blue).	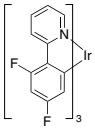	λ_{max} = 347 nm λ_{em} = 480 nm in chloroform	682594-250MG

Electronics and Self-Assembly with Single Molecules




Kasper Moth-Poulsen, Titoo Jain, Jakob Kryger Sørensen and Thomas Bjørnholm*
Nano-Science Center & Department of Chemistry, University of Copenhagen,
Universitetsparken 5, 2100 Copenhagen, Denmark
*E-mail: tb@nano.ku.dk

Introduction

Single molecule electronics is the endeavour of constructing electronic circuitry with single molecules as the fundamental building block. The concept has been addressed theoretically in the 1970s[1] and many experimental realizations of single molecule transistors have emerged since the middle of the 1990s.[2-4] The research is motivated both by a fundamental interest for electron transport on the nanometer length scale and by a vision of developing molecular self-assembled materials as an alternative to current top-down semiconductor technologies.[5,6] So far, most of the work in this field has focused on the development of test beds for the measurement of electronic transport through a single molecule. In a typical experiment, microscopic wires are fabricated by top-down lithographic techniques. The wires are later carefully broken, either mechanically or by applying a current strong enough to break the wires and leave a nanometer wide gap between the two wires.[7,8] The molecule of interest is then applied to the nanogap, either via the gas phase or via solution based self-assembly. The chemical bond to the electrode material (e.g. gold) is typically formed via mercapto or amino functional groups, often referred to as a chemical "alligator clips".[9] One of the lessons learned from these studies is that atomic precision of the interface between molecule and electrodes is of paramount importance: single atom changes in contact geometry can change the conducting properties of a single molecule by up to 5 orders of magnitude.[10] Modern silicon based computer chips consist of 10^6-10^9 active components, yet molecular electronics with single molecules are at a stage where it is challenging to make reproducible measurements on the single device level. Major improvements in device fabrication methods and in the way the molecules are contacted to the electrodes are therefore needed. One of the challenges in the field is therefore to develop methods that allow for the integration of multiple molecular components in a single experimental realization. In this report we present some of the emerging methods for self-assembly of single molecule circuitry together with concepts for the chemical control of the interface between molecule and electrode based on the recent work at the Copenhagen University Nano-Science Center.[4,10-16]

Self-assembly at the Air-Water Interface

Self-assembly at the air-water interface, facilitated using the so-called Langmuir-Blodgett (LB) technique, is a well established method that has revealed much knowledge of the inherent behavior of both molecules and nanoparticles. The technique involves the use of amphiphilic molecules that form a monolayer at the water-air interface. By adjusting the surface tension the molecules are forming 2-dimensional architectures which are readily studied by a handful of techniques such as X-ray reflectometry, grazing incidence X-rays, or simply by scanning probe techniques. Gold nanoparticles have become popular building blocks for various nanoscale assemblies.[6,16] Here, 1-2 nm gold nanoparticles were prepared by the so-called Brust method, which is the reduction of Au(III) by $NaBH_4$ in a two phase system in the presence of a protecting thiol, typically dodecane thiol (**Aldrich Prod. No. 471364**).[17] In an effort to construct gold nanowires by self-assembly the gold nanoparticles were spread on a water surface in a Langmuir-Blodgett trough. When co-spread with a suitable surfactant, such as DPPC[18] (**Aldrich Prod. No. D206555**) or ambipolar polymers,[12] the gold nanoparticles are organized into wires or maze structures (**Figure 1**). Subjecting the assembled wire structures to solutions of oligo(phenylene-vinylene)s (OPVs) allows for electronic characterization, and therefore an estimate of the single molecule conductances.[13] The prospects of using the air-water interface for the self-assembly of inorganic nanoparticles is further exploited in a recent review by Tao *et al.*[19]

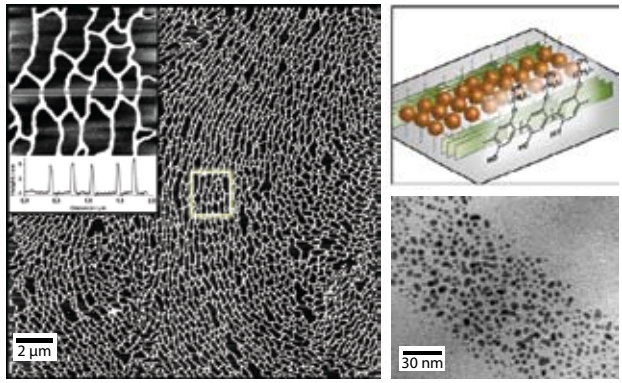

Figure 1. Self-assembled maze structures of gold nanoparticles. The structures were assembled at the air-water interface by co-spreading gold nanoparticles together with an amphiphilic polymer. AFM overview of the maze structure (left), illustration of the self-assembly process (top right) and high resolution TEM of a wire consisting of gold nanoparticles.[12]

Self-assembled Nanogaps with a Single Molecule Incorporated

One of the important challenges in molecular electronics is the preparation of a 1-2 nm nanogap with a single molecule situated in the nanogap. In a recent report, gold nanorods were used to bridge the gap between the molecular length scale (1-2 nm) and the micrometer length scale, which is readily accessible by simple lithographic techniques.[11] Gold nanorods have recently attracted large interest due to their ease of synthesis, unique shape dependant optical properties, and possible biochemical imaging[20] and medical applications.[21] The most widely used preparation method is the seed-mediated and surfactant assisted synthesis, first reported by Murphy and co-workers.[22] In brief, citrate-stabilized gold nanoparticle seeds are prepared by the reduction of $HAuCl_4$ (**Aldrich Prod. No. 484385**) with $NaBH_4$ (**Aldrich Prod. No. 480886**) in an aqueous citrate solution. The seeds are then added to a growth solution containing the surfactant CTAB (**Aldrich Prod. No. H9151**), $HAuCl_4$ and ascorbic acid (**Aldrich Prod. No. A5960**). Depending on the specific growth conditions and purification schemes, rods with aspect ratios from 4 to 25 can be prepared.[23,24] Important factors for the successful synthesis are the use of the correct type of CTAB surfactant[25] (**Aldrich batch H6269**), precise temperature control and clean glassware. Gold nanorod dimers can be prepared by addition of a water soluble thiol end-functionalized polyethylene glycol (HS-PEG-SH) to the gold nanoparticle seeds before they are exposed to the growth conditions. By carefully tuning the concentration of HS-PEG-SH the reaction conditions are optimized to yield a high degree of gold nanorod dimers. By diluting the HS-PEG-SH concentration further, one can, to a high degree, expect that a single molecule is acting as the linker between two nanorods (**Figure 2**).[11]

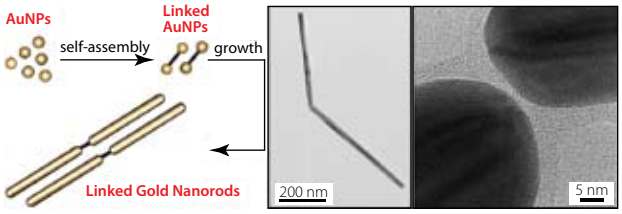

Figure 2. Scheme depicting the synthesis of linked gold nanords (left). TEM images of linked gold nanorods at different magnifications (right).[11]

In another experiment (**Figure 3**), the electronic properties of the gold rods were tested. First, gold nanorods were self-assembled to gold nanoparticle-coated tin oxide nanowires. The assembly was facilitated using thiol end-capped oligo(phenylenevinylene)s (OPVs) which are interesting test molecules exceeding low tunneling barriers[26] and widely used in molecular electronic experiments.[4,10] Second, the electronic properties of the OPV molecule were probed by conducting atomic force microscopy (C-AFM). The conductive AFM tip was placed directly on the gold nanorod as one electrode, while the much larger tin oxide nanowire acted as the second electrode, which was easily connected to close the electronic circuit around the molecule (**Figure 3**). *I-V* characteristics revealed signatures similar to those previously obtained for OPV molecules, thus also confirming that gold nanorods may be promising candidates for bridging the gap between the molecular and micrometer length scale.

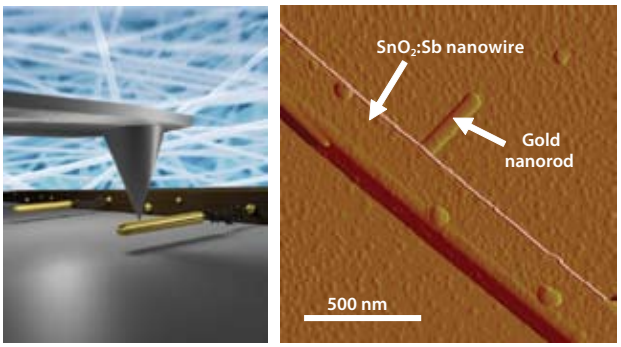

Figure 3. Artistic impression of the measuring of a single or a few molecules via a conducting AFM tip (left) and AFM picture (right) of gold nanorods self-assembled to tin oxide nanowires mediated by thiol end-capped oligo(phenylenevinylene) molecules.[14]

Synthesis of a Conducting Molecule with Well Defined Contact Geometry

Control of the contact between a molecule and the electrode surface has proved challenging since minute changes in atomic position of the binding thiol or the atomic structure of the surface may lead to large difference in the electronic properties.[27] In an attempt to circumvent the challenges discussed above, C_{60} was introduced as an alternative anchoring group. The C_{60} molecule can create a strong contact to the surface through multiple connection sites, thus rendering the details of the contact site less important since the limiting tunneling barrier is now moved from the interface between molecule and electrode to well defined chemical bonds inside the molecule. As a consequence, the detailed contact geometry can then be controlled by chemical synthesis of C_{60} derivatives (**Figure 4**). The first electronic measurements taking use of this concept was described by Martin *et al.*[15] who performed single molecule measurements using the break junction technique, and found that one of the dominant features of the molecule was extremely high stability of the single molecule junctions - even at room temperature.

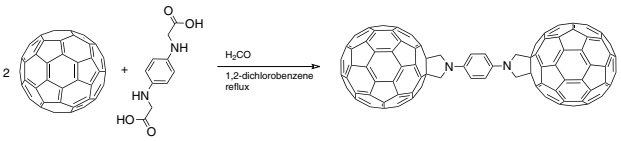

Figure 4. Synthesis of a Würster's blue derivative with C_{60} alligator clips.[15]

The C_{60}-anchored molecule (1,4-bis(fullero[*c*]pyrrolidin-1-yl)benzene) was synthesized via [2+3]cycloaddition reaction of an in situ generated azomethine ylide to a fullerene carbon-carbon double bond. This reaction is known as the Prato-reaction.[28] In brief, *N,N'*-(1,4-phenylene) bisglycine and paraformaldehyde (**Aldrich Prod. No. 16005**) was sonicated in 1,2-dicholorbenzene (**Aldrich Prod. No. 240664**) and added to a solution of C_{60} in 1,2-dichlorobenzene. The reaction mixture was refluxed for 6 hours yielding the black target molecule in 28% yield after purification (**Figure 4**).[15]

Conclusion

In order to be able to study the intrinsic charge transport mechanisms in individual molecules, one of the main challenges is to circumvent problems associated with the specific position of the bonds between electrodes and molecules. A strategy for predefining the metal-molecule interface, and thereby achieving atomic scale precision, by the introduction of new C_{60}-based anchoring groups have been presented. Another challenge is the fact that only one molecular junction is realized per device, hence the realization of molecular circuitry with numerous individual addressable components is highly desirable. Alternative routes that may help overcome these challenges are the use of chemical bottom-up fabrication techniques such as the Langmuir-Blodgett technique or other self-assembly based methods that may aid in the development towards complex circuitry. One possibility is the bottom-up synthesis of electrodes (gold nanorods) with molecules incorporated directly in the nanogap and prepared by the use of simple aqueous solution-based chemistries.

References:

(1) Aviram, A; Ratner, M. A. *Chem Phys. Lett.* **1974**, *29,* 277-283.
(2) Reed, M. A.; Zhou, C.; Muller, C. J.; Burgin, P.; Tour, J. M. *Science* **1997**, *278,* 252-254
(3) Joachim, C.; Gimzewski, J. K.; Schlittler, R. R.; Chavy, C. *Phys. Rev. Lett.,* **1995**, *74,* 2102-2105.
(4) Moth-Poulsen, K.; Bjørnholm, T. *Nature Nanotech* **2009**, *4(9), 551-556.*
(5) Smits, E. S. G. *et al. Nature,* **2008**, *455,* 956-959.
(6) Westerlund, F.; Bjørnholm, T. *Curr. Opin. Colloid In.* **2009**, *14,* 126-134.
(7) Martin, C. A.; Ding, D.; van der Zant, H. S. J.; van Ruitenbeek, J. M. *New J. Phys.* **2008**, *10,* 065008.
(8) Prokopuk, N.; Son, K-A. *J. Phys.: Condens. Matter* **2008**, *20,* 374116.
(9) Pearson, D. L.; Tour, J. M. *J. Org. Chem.* **1997**, *62* (5), 1376-1387.
(10) Danilov, A.; Kubatkin, S.; Kafanov, S.; Hedegard, P.; Stuhr-Hansen, N.; Moth-Poulsen, K; Bjørnholm, T. *Nano Letters* **2008**, *8* (1) 1-5.
(11) Jain, T.; Westerlund, F.; Johnson, E.; Moth-Poulsen, K.; Bjørnholm, T. *ACS Nano.* **2009**, *3* (4), 828-834
(12) Hansen, C.; Westerlund, F.; Moth-Poulsen, K.; Ravindranath, R.; Valiyaveettil, S.; Bjørnholm, T. *Langmuir* **2008**, *24,* 3905-3910.
(13) Hassenkam, T.; Moth-Poulsen, K.; Stuhr-Hansen, N.; Nørgaard, K.; Kabir, M. S.; Bjørnholm, T. *Nano Letters* **2004**, *4* (1).
(14) Tang, Q.; Tong, Y.; Jain, T.; Hassenkam, T.; Wan, Q.; Moth-Poulsen, K.; Bjørnholm, T. *Nanotechnology* **2009**, *20* (24), 245205
(15) Martin, C. A.; Ding, D.; Sørensen, J. K.; Bjørnholm, T.; van Ruitenbeek, J. M.; van der Zant, H. S. J. *J. Am. Chem. Soc.* **2008**, *130,* 13198-13199.
(16) Nørgaard, K.; Bjørnholm, T. *Chem. Commun.* **2005**, 1812.
(17) Brust, M.; Walker, M.; Bethell, D.; Schiffrin, D. J.; Whyman, R. *J. Chem. Soc., Chem. Commun.* **1994**, 801.
(18) Hassenkam, T.; Nørgaard, K.; Iversen, L.; Kiely, C. J.; Brust, M.; Bjørnholm, T. *Adv. Mater.* **2002**, *14*, 1126.
(19) Tao, A. R.; Huang, J. X.; Yang, P. D. *Acc. Chem. Res.* **2008**, *41* (12) 1662-1673.
(20) Murphy, C. J.; Gole, A. M.; Hunyadi, S. E.; Stone, J. W.; Sisco, P. N.; Alkilany, A., *Chem. Commun.* **2008**, *5*, 544–557.
(21) Huang, X.; Jain, P. K.; El-Sayed, I. H.; El-Sayed, M. A. *Lasers Med. Sci.* **2008**, *23*, 217–228.
(22) Jana, N. R.; Gearheart, L.; Murphy, C. J. *Adv. Mater.* **2001**, *13*, 1389–1393.
(23) Gao, J.; Bender, C. M.; Murphy, C. J. *Langmuir* **2003**, *19*, 9065–9070. 10
(24) Grzelczak, M.; Perez-Juste, J.; Mulvaney, P.; Liz-Marzan, L. M. *Chem. Soc. Rev.* **2008**, *37*, 1783–1791.
(25) Smith, D. K.; Korgel, B. A. *Langmuir* **2008,** *24,* 644-649
(26) Moth-Poulsen, K.; Patrone, L.; Stuhr-Hansen, N.; Christensen, J. B.; Bourgoin J.-P.; Bjørnholm, T. *Nano Lett.* **2005,** *5* (4): 783-785.
(27) (a) Moore, A. M.; Dameron, A. A.; Mantooth, B. A.; Smith, R. K.; Fuchs, D. J.; Ciszek, J. W.; Maya, F.; Yao, Y.; Tour, J. M.; Weiss, P. S. *J. Am. Chem. Soc.* **2006**, *128*, 1959–1967. (b) Ulrich, J.; Esrail, D.; Pontius, W.; Venkataraman, L.; Millar, D.; Doerrer, L. H. *J. Phys. Chem. B* **2006**, *110*, 2462–2466. (c) Li, C.; Pobelov, I.; Wandlowski, T.; Bagrets, A.; Arnold, A.; Evers, F. *J. Am. Chem. Soc.* **2008**, *130*, 318–326.
(28) Maggini, M.; Scorrano, G.; Prato, M. *J. Am. Chem. Soc.* **1993**, *115*, 9798–9799

Self-Assembly Materials

A comprehensive library of self-assembly materials can be viewed at ***sigma-aldrich.com/self-assembly***

Monofunctional Thiols

Name	Chain Length	Structure	Purity/Concentration	Cat. No.
Cyclohexanethiol	■	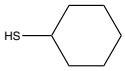	97%	C105600-25G C105600-100G
m-Carborane-9-thiol	■	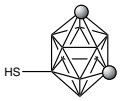	97%	686506-250MG
m-Carborane-1-thiol	■	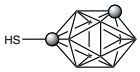	96%	695572-250MG
1-Adamantanethiol	■	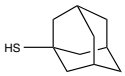	95%	659452-5G
NanoThinks™ 8	■	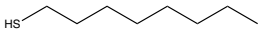	5 mM in ethanol	662208-100ML
1-Decanethiol	■	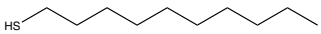	99%	705233-1G
1,1′,4′,1″-Terphenyl-4-thiol	■	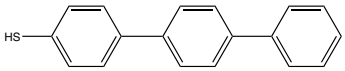	97%	708488-500MG
1-Dodecanethiol	■	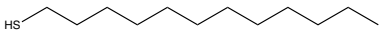	≥98%	471364-100ML 471364-500ML 471364-2L 471364-18L

Chain Length Key: ■ **0–5** ■ **6–10** ■ **11–15** ■ **16+**

Name	Chain Length	Structure	Purity/Concentration	Cat. No.
1-Hexadecanethiol	■	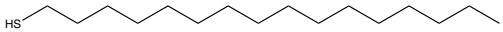	99%	674516-500MG
NanoThinks™ 18	■	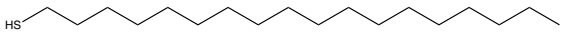	5 mM in ethanol	662194-100ML
(11-Mercaptoundecyl) tri(ethyleneglycol) monomethyl ether	■	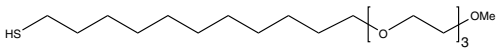	≥95%	717002-250MG
(11-Mercaptoundecyl) hexa(ethylene glycol) monomethyl ether	■	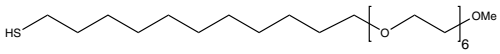	≥95%	716995-250MG

Bifunctional Molecules

Name	Chain Length	Structure	Purity/Concentration	Cat. No.
3-Mercaptopropionic acid	■	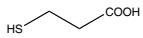	≥99%	M5801-5G M5801-100G M5801-500G
3-Mercapto-1-propanol	■	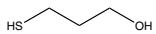	95%	405736-1G 405736-5G
1,4-Butanedithiol	■	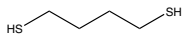	97%	B85404-5G B85404-25G
4-Cyano-1-butanethiol	■	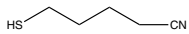	97%	692581-500MG
1,6-Hexanedithiol	■	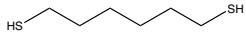	96%	H12005-5G H12005-25G
8-Mercaptooctanoic acid	■	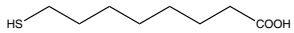	95%	675075-1G
NanoThinks™ THIO8	■	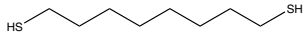	5 mM in ethanol	662615-100ML
8-Mercapto-1-octanol	■	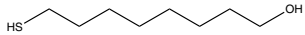	98%	706922-1G
2,2′-(Ethylenedioxy) diethanethiol	■	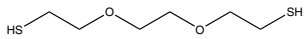	95%	465178-100ML 465178-500ML
4,4′-Dimercaptostilbene	■	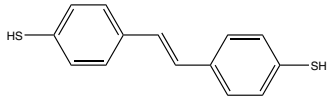	>96%	701696-100MG
6-(Ferrocenyl)hexane-thiol	■	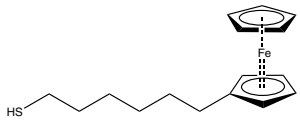	-	682527-250MG
11-Bromo-1-undecanethiol	■		99%	701335-250MG
11-Amino-1-undecanethiol hydrochloride	■	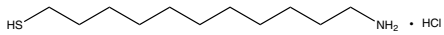	99%	674397-50MG
11-Mercapto-1-undecanol	■	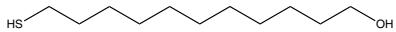	99%	674249-250MG
12-Mercapto-dodecanoic acid	■	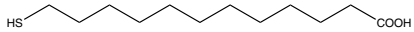	99%	705241-500MG
p-Terphenyl-4,4″-dithiol	■	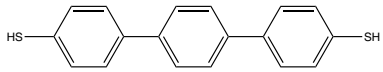	96%	704709-1G
NanoThinks™ ACID16	■	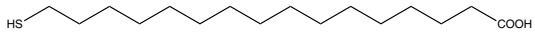	5 mM in ethanol	662216-100ML
Triethylene glycol mono-11-mercaptoundecyl ether	■	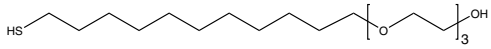	95%	673110-250MG
(11-Mercaptoundecyl) tetra(ethylene glycol)	■	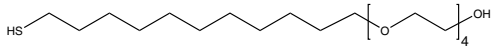	95%	674508-250MG
(11-Mercaptoundecyl) hexa(ethylene glycol)	■	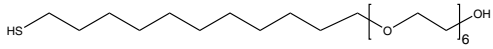	95%	675105-250MG

Chain Length Key: ■ **0–5** ■ **6–10** ■ **11–15** ■ **16+**

Protected Thiols for In-situ Deprotection

Name	Chain Length	Structure	Purity	Cat. No.
S-(4-Cyanobutyl) thioacetate	■	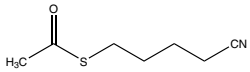	97%	694754-1G
1,4-Butanedithiol diacetate	■	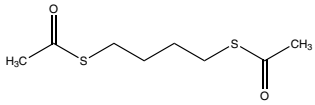	97%	558826-1G 558826-5G
S-(11-Bromoundecyl) thioacetate	■	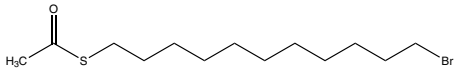	95%	706930-1G
S-[4-[2-[4-(2-Phenyl-ethynyl)phenyl]ethynyl] phenyl] thioacetate	■	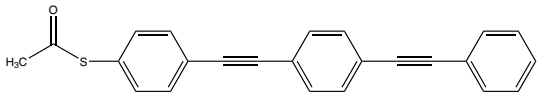	≥95%	718378-100MG
S,S'-[1,4-Phenylenebis(2,1-ethynediyl-4,1-phenylene)] bis(thioacetate)	■	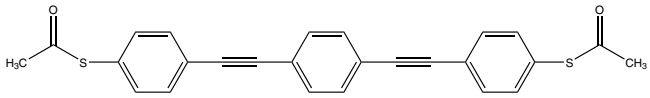	≥95%	718351-100MG
[11-(Methyl-carbonylthio)undecyl] tetra(ethylene glycol)	■	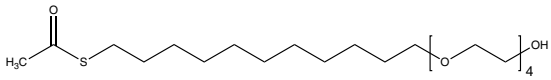	95%	674176-250MG
Hexa(ethylene glycol) mono-11-(acetylthio) undecyl ether	■	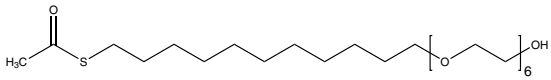	95%	675849-250MG

Chain Length Key: ■ **0–5** ■ **6–10** ■ **11–15** ■ **16+**

Gold Nanostructures

Nanoparticles

Name	Physical Form	Particle Size (nm)	Cat. No.
Gold	nanopowder, $HAuCl_4$	particle size <100	636347-1G
Gold colloid	dispersion nanoparticles, ~ 0.01% ~ 1 A_{520} units/mL	mean particle size 17 - 23 (monodisperse) particle size 20	G1652-25ML
	dispersion nanoparticles, ~ 0.01% ~ 1 A_{520} units/mL	mean particle size 8.5 - 12.0 (monodisperse) particle size 10	G1527-25ML
	dispersion nanoparticles, ~ 0.01% ~ 1 A_{520} units/mL	mean particle size 3.0 - 5.5 (monodisperse) particle size 5	G1402-25ML
Octanethiol functionalized gold nanoparticles	solution, 2 % (w/v) in toluene	particle size 2 - 4 DLS)	660426-5ML
Dodecanethiol functionalized gold nanoparticles	solution, 2 % (w/v) in toluene	particle size 3 - 5 TEM)	660434-5ML
	dispersion, 0.01% in toluene	particle size 3 - 6	54349-10ML-F

Bare Nanorods

Name	Absorption	Physical Form	Diam. × L (nm)	Cat. No.
Gold nanorods	780 nm	dispersion, 35 µg/mL in H_2O	10 × 38	716812-25ML
	808 nm	dispersion, 36 µg/mL in H_2O	10 × 41	716820-25ML
	850 nm	dispersion, 35 µg/mL in H_2O	10 × 45	716839-25ML
	550 nm	dispersion, 171 µg/mL in H_2O	25 × 34	716847-25ML
	600 nm	dispersion, 235 µg/mL in H_2O	25 × 44	716855-25ML
	650 nm	dispersion, 150 µg/mL in H_2O	25 × 60	716863-25ML
Gold microrods	-	dispersion, 50 µg/mL in H_2O	200 × 1000	716960-10ML

Functionalized Nanorods

Name	Absorption	Physical Form	Diam. × L (nm)	Cat. No.
Gold nanorods, amine terminated	808 nm	dispersion, 0.9 mg/mL in H_2O	10 × 41	716871-1ML
Gold nanorods, carboxyl terminated	808 nm	dispersion, 0.9 mg/mL in H_2O	10 × 41	716898-1ML
Gold nanorods, methyl terminated	808 nm	dispersion, 0.9 mg/mL in H_2O	10 × 41	716901-1ML

Catalytic Nanorods

Name	Absorption	Physical Form	Diam. × L (nm)	Cat. No.
Gold nanorods, palladium coated	700 nm	dispersion, 100 µg/mL in H_2O	25 × 75	716928-10ML
Gold nanorods, platinum coated	700 nm	dispersion, 100 µg/mL in H_2O	25 × 75	716936-10ML

Nanowires

Name	Physical Form	Diam. × L (nm)	Cat. No.
Gold nanowires	dispersion, 0.6 mg/mL in H_2O	30 × 4,500	716944-10ML
	dispersion, 0.5 mg/mL in H_2O	30 × 6,000	716952-10ML

Gold Nanoparticle Precursors

Chemical Structure	Name	Cat. No.
$AuCl_3$	Gold(III) chloride, ≥99.99% trace metals basis	379948-250MG 379948-1G
$HAuCl_4$	Gold(III) chloride, 99.99% trace metals basis	484385-10G 484385-50G
$HAuCl_4 \cdot xH_2O$	Gold(III) chloride, 99.999% trace metals basis	254169-500MG 254169-5G
$HAuCl_4 \cdot 3H_2O$	Gold(III) chloride, ≥99.9% trace metals basis	520918-1G 520918-5G 520918-25G
$AuCl_4K$	Potassium gold(III) chloride, 99.995% trace metals basis	450235-250MG 450235-1G

Sigma-Aldrich
3050 Spruce Street
St. Louis, MO 63103 USA
sigma-aldrich.com

Argentina
SIGMA-ALDRICH DE ARGENTINA S.A.
Free Tel: 0810 888 7446
Tel: (+54) 11 4556 1472
Fax: (+54) 11 4552 1698

Australia
SIGMA-ALDRICH PTY LTD.
Free Tel: 1800 800 097
Free Fax: 1800 800 096
Tel: (+61) 2 9841 0555
Fax: (+61) 2 9841 0500

Austria
SIGMA-ALDRICH HANDELS GmbH
Tel: (+43) 1 605 81 10
Fax: (+43) 1 605 81 20

Belgium
SIGMA-ALDRICH NV/S.A.
Free Tel: 0800 14747
Free Fax: 0800 14745
Tel: (+32) 3 899 13 01
Fax: (+32) 3 899 13 11

Brazil
SIGMA-ALDRICH BRASIL LTDA.
Free Tel: 0800 701 7425
Tel: (+55) 11 3732 3100
Fax: (+55) 11 5522 9895

Canada
SIGMA-ALDRICH CANADA LTD.
Free Tel: 1800 565 1400
Free Fax: 1800 265 3858
Tel: (+1) 905 829 9500
Fax: (+1) 905 829 9292

Chile
SIGMA-ALDRICH
QUIMICA LIMITADA
Tel: (+56) 2 495 7395
Fax: (+56) 2 495 7396

China
SIGMA-ALDRICH (SHANGHAI)
TRADING CO. LTD.
Free Tel: 800 819 3336
Tel: (+86) 21 6141 5566
Fax: (+86) 21 6141 5567

Czech Republic
SIGMA-ALDRICH spol. s r. o.
Tel: (+420) 246 003 200
Fax: (+420) 246 003 291

Denmark
SIGMA-ALDRICH DENMARK A/S
Tel: (+45) 43 56 59 00
Fax: (+45) 43 56 59 05

Finland
SIGMA-ALDRICH FINLAND OY
Tel: (+358) 9 350 9250
Fax: (+358) 9 350 92555

France
SIGMA-ALDRICH CHIMIE S.à.r.l.
Free Tel: 0800 211 408
Free Fax: 0800 031 052
Tel: (+33) 474 82 28 00
Fax: (+33) 474 95 68 08

Germany
SIGMA-ALDRICH CHEMIE GmbH
Free Tel: 0800 51 55 000
Free Fax: 0800 64 90 000
Tel: (+49) 89 6513 0
Fax: (+49) 89 6513 1160

Greece
SIGMA-ALDRICH (O.M.) LTD.
Tel: (+30) 210 994 8010
Fax: (+30) 210 994 3831

Hungary
SIGMA-ALDRICH Kft
Ingyenes telefonszám: 06 80 355 355
Ingyenes fax szám: 06 80 344 344
Tel: (+36) 1 235 9055
Fax: (+36) 1 235 9050

India
SIGMA-ALDRICH CHEMICALS
PRIVATE LIMITED
Telephone
Bangalore: (+91) 80 6621 9400
New Delhi: (+91) 11 4358 8000
Mumbai: (+91) 22 2570 2364
Hyderabad: (+91) 40 4015 5488
Kolkata: (+91) 33 4013 8003
Fax
Bangalore: (+91) 80 6621 9650
New Delhi: (+91) 11 4358 8001
Mumbai: (+91) 22 2579 7589
Hyderabad: (+91) 40 4015 5466
Kolkata: (+91) 33 4013 8016

Ireland
SIGMA-ALDRICH IRELAND LTD.
Free Tel: 1800 200 888
Free Fax: 1800 600 222
Tel: (+353) 402 20370
Fax: (+ 353) 402 20375

Israel
SIGMA-ALDRICH ISRAEL LTD.
Free Tel: 1 800 70 2222
Tel: (+972) 8 948 4100
Fax: (+972) 8 948 4200

Italy
SIGMA-ALDRICH S.r.l.
Numero Verde: 800 827018
Tel: (+39) 02 3341 7310
Fax: (+39) 02 3801 0737

Japan
SIGMA-ALDRICH JAPAN K.K.
Tel: (+81) 3 5796 7300
Fax: (+81) 3 5796 7315

Korea
SIGMA-ALDRICH KOREA
Free Tel: (+82) 80 023 7111
Free Fax: (+82) 80 023 8111
Tel: (+82) 31 329 9000
Fax: (+82) 31 329 9090

Malaysia
SIGMA-ALDRICH (M) SDN. BHD
Tel: (+60) 3 5635 3321
Fax: (+60) 3 5635 4116

Mexico
SIGMA-ALDRICH QUÍMICA, S.A. de C.V.
Free Tel: 01 800 007 5300
Free Fax: 01 800 712 9920
Tel: (+52) 722 276 1600
Fax: (+52) 722 276 1601

The Netherlands
SIGMA-ALDRICH CHEMIE BV
Free Tel: 0800 022 9088
Free Fax: 0800 022 9089
Tel: (+31) 78 620 5411
Fax: (+31) 78 620 5421

New Zealand
SIGMA-ALDRICH NEW ZEALAND LTD.
Free Tel: 0800 936 666
Free Fax: 0800 937 777
Tel: (+61) 2 9841 0555
Fax: (+61) 2 9841 0500

Norway
SIGMA-ALDRICH NORWAY AS
Tel: (+47) 23 17 60 00
Fax: (+47) 23 17 60 10

Poland
SIGMA-ALDRICH Sp. z o.o.
Tel: (+48) 61 829 01 00
Fax: (+48) 61 829 01 20

Portugal
SIGMA-ALDRICH QUÍMICA, S.A.
Free Tel: 800 202 180
Free Fax: 800 202 178
Tel: (+351) 21 924 2555
Fax: (+351) 21 924 2610

Russia
SIGMA-ALDRICH RUS, LLC
Tel: (+7) 495 621 5579
Fax: (+7) 495 621 5923

Singapore
SIGMA-ALDRICH PTE. LTD.
Tel: (+65) 6779 1200
Fax: (+65) 6779 1822

Slovakia
SIGMA-ALDRICH spol. s r. o.
Tel: (+421) 255 571 562
Fax: (+421) 255 571 564

South Africa
SIGMA-ALDRICH (PTY) LTD.
Free Tel: 0800 1100 75
Free Fax: 0800 1100 79
Tel: (+27) 11 979 1188
Fax: (+27) 11 979 1119

Spain
SIGMA-ALDRICH QUÍMICA, S.A.
Free Tel: 900 101 376
Free Fax: 900 102 028
Tel: (+34) 91 661 99 77
Fax: (+34) 91 661 96 42

Sweden
SIGMA-ALDRICH SWEDEN AB
Tel: (+46) 8 742 4200
Fax: (+46) 8 742 4243

Switzerland
SIGMA-ALDRICH CHEMIE GmbH
Free Tel: 0800 80 00 80
Free Fax: 0800 80 00 81
Tel: (+41) 81 755 2828
Fax: (+41) 81 755 2815

United Kingdom
SIGMA-ALDRICH COMPANY LTD.
Free Tel: 0800 717 181
Free Fax: 0800 378 785
Tel: (+44) 1747 833 000
Fax: (+44) 1747 833 313

United States
SIGMA-ALDRICH
Toll-Free: 800 325 3010
Toll-Free Fax: 800 325 5052
Tel: (+1) 314 771 5765
Fax: (+1) 314 771 5757

Vietnam
SIGMA-ALDRICH PTE LTD. VN R.O.
Tel: (+84) 3516 2810
Fax: (+84) 6258 4238

Internet
sigma-aldrich.com

World Headquarters
3050 Spruce St., St. Louis, MO 63103
(314) 771-5765
sigma-aldrich.com

Order/Customer Service (800) 325-3010 • Fax (800) 325-5052
Technical Service (800) 325-5832 • *sigma-aldrich.com/techservice*
Development/Custom Manufacturing Inquiries SAFC® (800) 244-1173
Safety-related Information *sigma-aldrich.com/safetycenter*

Accelerating Customers' Success through Innovation and Leadership in ***Life Science, High Technology*** *and* ***Service***

LSU
72175-508473
0109

SIGMA-ALDRICH®